



Where Moon Bases Become Reality

Report I

June 15, 2023

1. Introduction

This report focuses on the careful selection of potential sites for the long anticipated establishment of human-built lunar colonies, often termed as *lunar villages*. The report also analyzes potential landing sites being presented by the Global Exploration Roadmap (2018) including those selected by NASA and other space agencies under several considerations.

2. Lunar Geology

Over a diverse range of features that constitute the geology of the moon, reported and analyzed from the past lunar missions, we have listed out the relevant geological features documented by the International Astronomical Union (IAU) for the analysis, which would eventually unravel some of the ideal sites for future exploration and research.

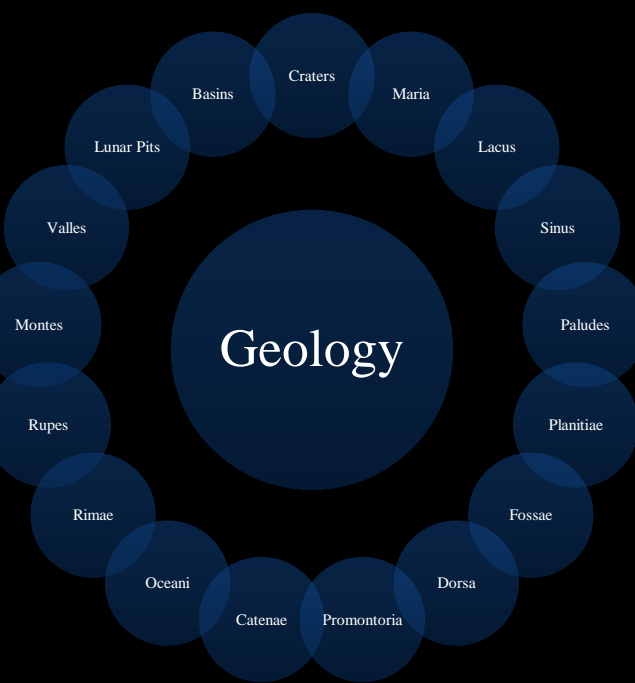


Figure 1: All lunar features.

For all of the features analyzed, we have laid down a set of standards which must be satisfied by the site in question to qualify as an ideal base location. These standards include:

- The site must be in proximity to the lunar south pole, because of stirring evidences of water ice in the PSRs of the lunar poles, detected by Moon Mineralogy Mapper (M3) instrument aboard the Chandrayan I spacecraft.

These ice deposits are patchily distributed and could possibly be ancient. At the southern pole, most of the ice is concentrated at lunar craters, while the northern pole's ice is more widely, but sparsely spread [1].

- The site must not lie within the permanently shadowed regions of the lunar surface.
- The site must be accessible, i.e. suitable for landing and exploration. For sites with similar characteristics, greater priority must be given to sites which have potential geological importance.

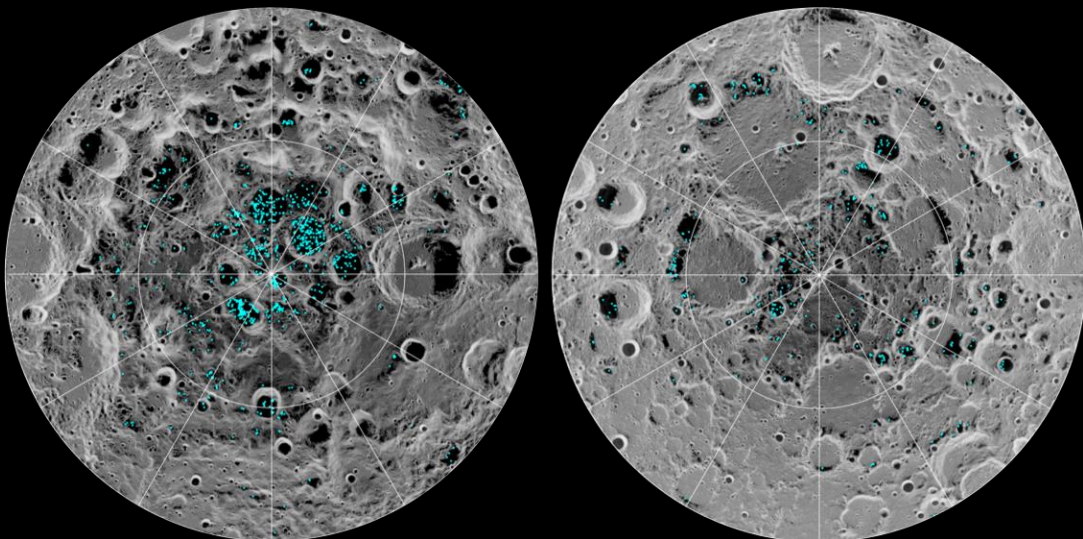


Figure 2: Distribution of surface ice on the lunar south pole (left) and north pole (right) [1]

3. Primary Analysis

In this section, we delve into the initial analysis of lunar features based on the data primarily from the former, yet important lunar missions like the Lunar Reconnaissance Orbiter by NASA. Based on the data reported by IAU, the latitudes of all the lunar features are planetocentric while the longitudes are planetographic. Thus with this important fact into consideration, we have implemented the haversine equation for computing the shortest distances between the potential sites and the lunar south pole, which serves as the primary standard for selection of potential base locations. This walkthrough shall also consider the sites put-forth by the international space agencies for future lunar explorations and analyze several smaller sites housed within the chosen sites that have the potential to establish some of the first colonies with the advantage of being much closer to the lunar south pole.

3.1. Craters

Lunar craters are mostly impact craters, i.e. they were caused by the asteroids and meteorites that collide with the lunar surface. The moon's surface is dotted with thousands of craters, thus searching for potential base locations amongst the instances of such widely abundant lunar feature is quite reasonable. Because of insignificant amounts of geological activity on the Moon, these craters remain intact for billions of years, thus lighting up the possibility of long-term settlement plans. This report analyzes a total of 1589 craters, adopted by the International Astronomical Union (IAU), and situated on both the near and far sides of the moon for an informed search of some of the best sites for human colonies with their proximity to the south pole as the benchmark for careful selection.

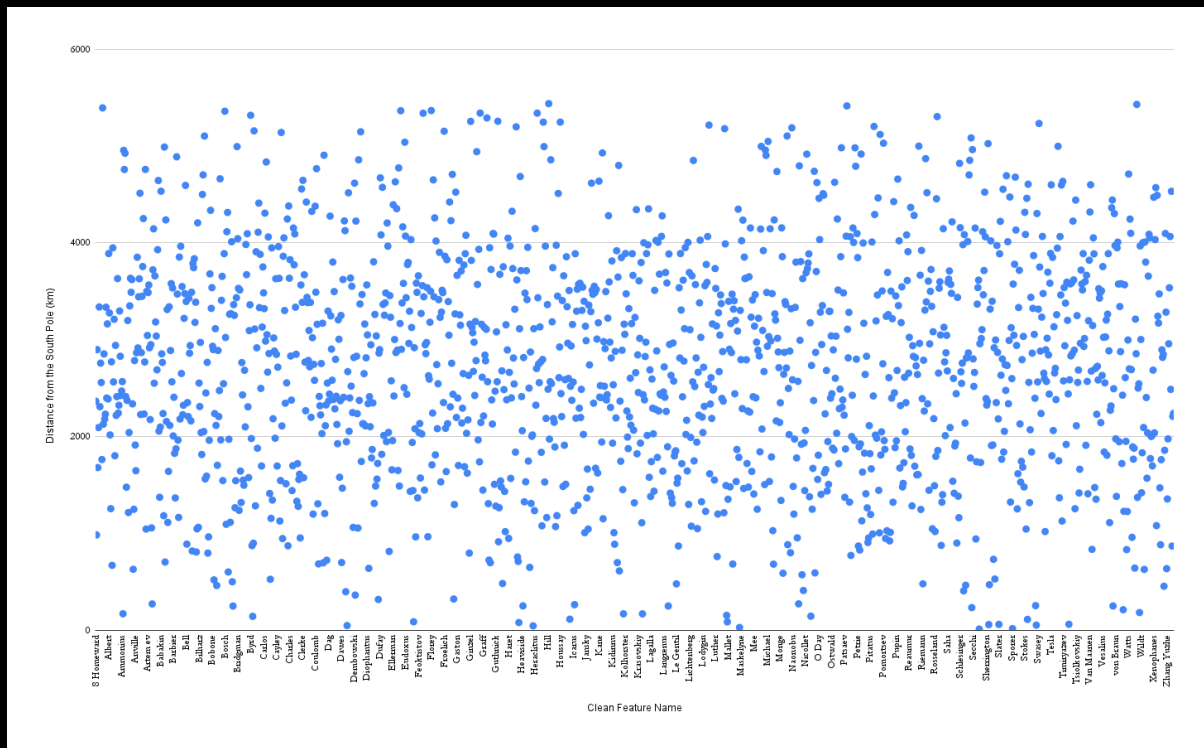


Figure 3: Scatterplot of the lunar impact craters signifying their distances from the south pole.

We shall revert back to the analysis of the impact craters after we have analyzed rest of the lunar features, owing to the fact that this very analysis and even beyond are deeply dependent on the analysis of lunar basins which shall come up in the following sections.

3.2. Maria

The lunar maria (or plains), which were formed between 3.1 and 3.9 billion years ago, are the youngest geologic units on the lunar surface, except for more recent impact craters [2]. The heat released from large impacts caused extensive melting and extrusion which led to the creation of dark basaltic plains. Thus, lunar maria are a feasible option for the search of potential base locations. We conducted an analysis on all of the officially recognized maria and estimated their haversine distances from the lunar south pole.

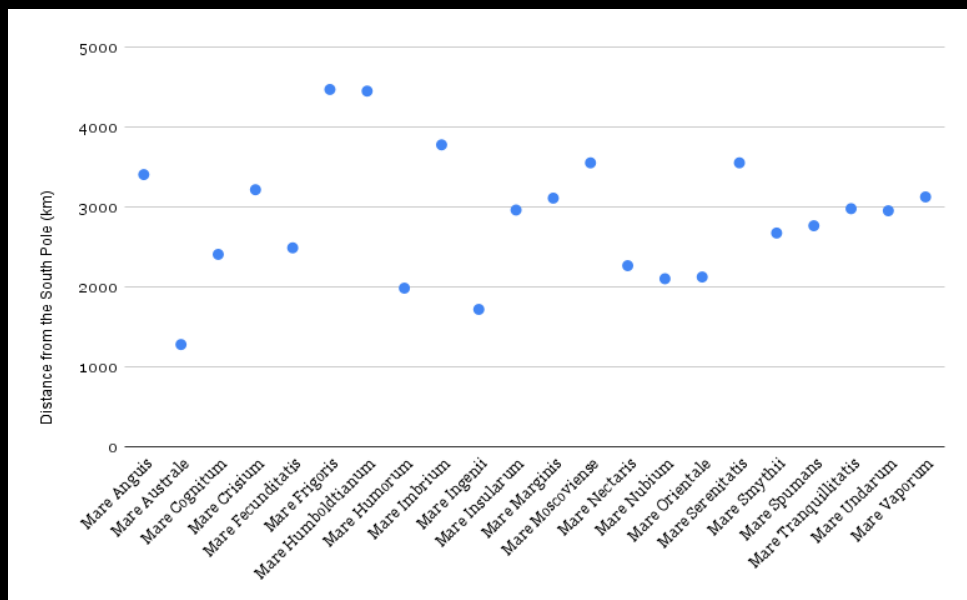


Figure 4: Plot of Maria with respect to their haversine distances from the South Pole.

In the light of our primary and most important standard which is crucial for an efficient and cost-effective base design, *Mare Australis* stands out, in terms of its unique features as well as its proximity to the lunar south pole, although miles distant metaphorically.

Mare Australis is located in the souther hemisphere, overlapping the near and far sides of the moon with its eastern half lying on the far side [3]. With a main ring diameter of about 880 km [4] and an overall diameter of 996.84 km [12], this mare houses numerous impact craters, resulting in its uneven surface.

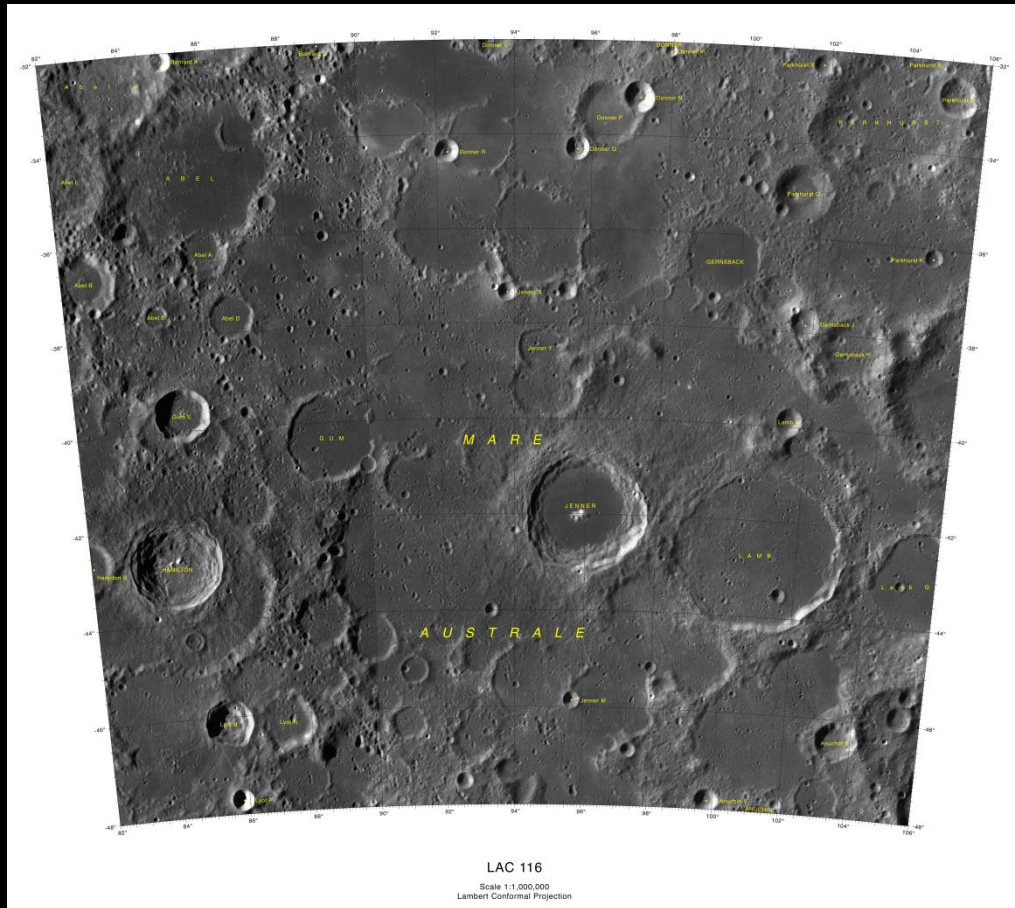


Figure 5: Lunar Quadrant with the center point of Mare Australe [12].

Based on the reported coordinates, we compute that the haversine distance between the lunar south pole and Mare Australe is approximately 1280.55508841183 km.

3.3. Lacus

Lunar *lacus* or “lakes” are smaller basaltic plains compared to the lunar maria. Being of similar origins, lunar lacus are worth analyzing, also taking into account the fact that this very lunar feature shall witness the first ever commercial mission to the Moon – Astrobotic’s Peregrine Mission One [6].

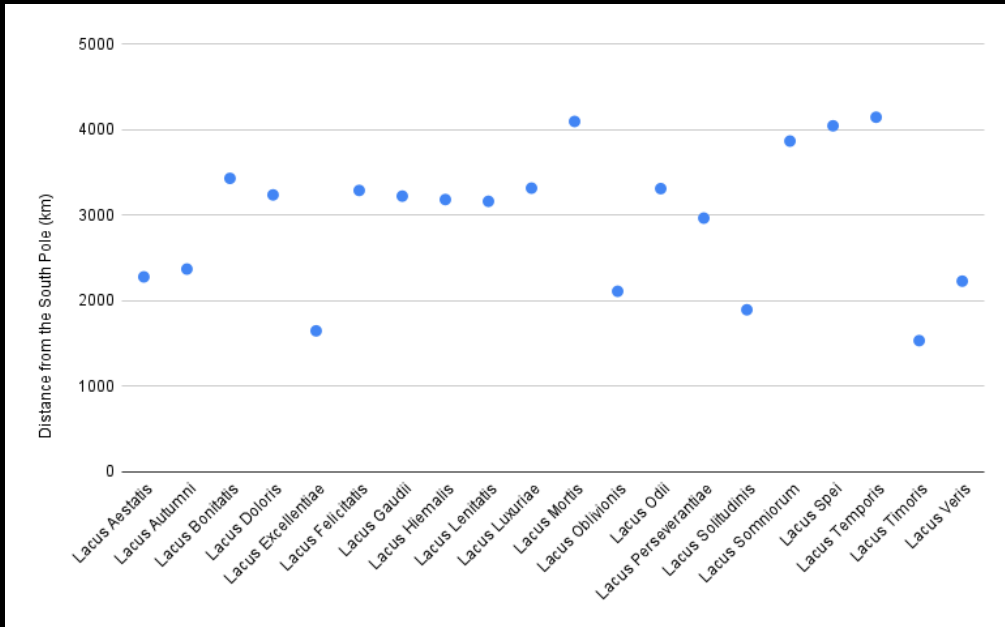


Figure 6: Scatter Plot of lacus with respect to their haversine distances from the South Pole.

Based on the computational output, we find Lacus Timoris to be the closest to the south pole. At a distance of 1533.75506445348 km from the south pole, Lacus Timoris is a small lunar mare with an approximate diameter of 153.65 km.

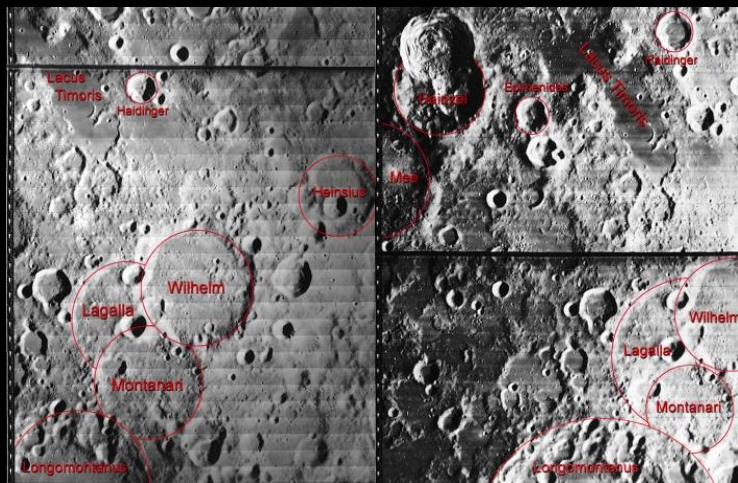


Figure 7: Location of Lacus Timoris w.r.t. nearby craters with photo center coordinates of 36.5°S/23.47°W (left) and 42.65°S/27.4°W (right) [5].

3.4. Sinus and Paludes

A distinct class of lunar features includes *sinus* and *paludes*, Latin for *bays* and *swamps* respectively, although the distinction between the duo is yet to be clearly laid out.

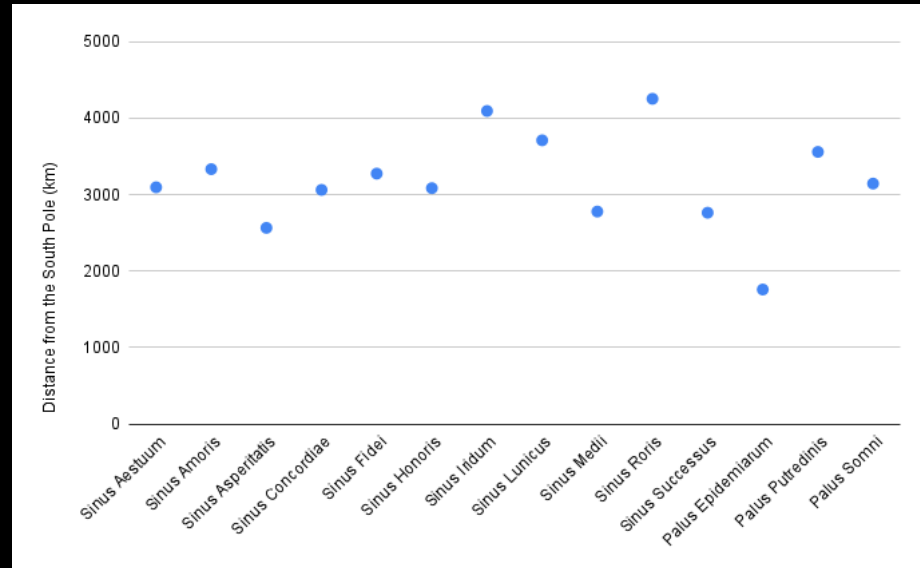


Figure 8: Scatter Plot of sinuses and paludes with respect to their haversine distances from the South Pole.

Taking into account the haversine distances to the lunar south pole, *Palus Epidemiarum* and *Sinus Asperitatis* are the closest, being approximately 1758.75432460067 km and 2565.0522123788 km respectively.

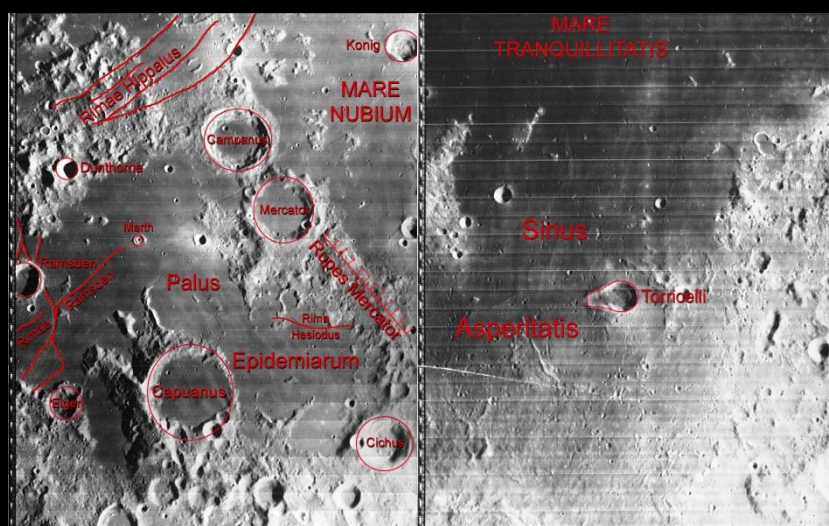


Figure 9: (Left) Palus Epidemiarum with image center coordinates $36.5^{\circ}\text{S}/23.47^{\circ}\text{W}$; (Right) Sinus Asperitatis with image center coordinates $14.93^{\circ}\text{S}/30.15^{\circ}\text{E}$ [5].

3.5. Planitiae

Lunar planitiae are one of the 18 different categories of lunar features recognized in the current system of IAU nomenclature. According to the IAU, a planitia is defined as a “low plain”. The only planitia that has been stated by the IAU is Planitia Descensus, *which was named to commemorate the site of the first soft landing of Luna 9* [13]. Planitia Descensus, with planetocentric center latitude of 7.18° and planetographic center longitude of -64.15° , is at a distance of approximately 2946.8231942188468 km from the lunar south pole.

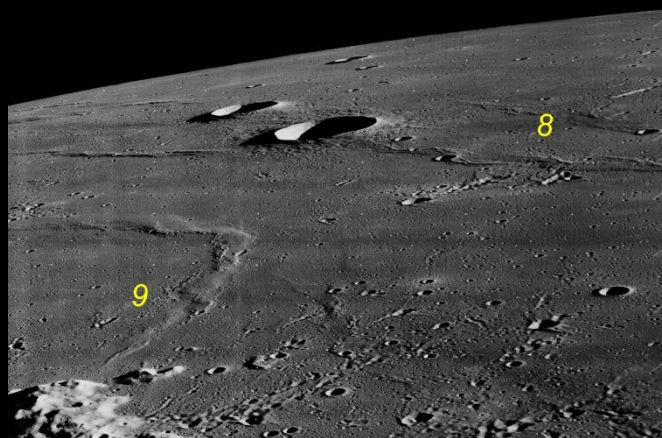


Figure 10: Oblique view, facing north. Galilaei crater is the largest crater above center. 8 and 9 represent landing spots of Luna 8 and 9 respectively.

3.7. Fossae

In planetary nomenclature, a fossa is a long, narrow depression (trough) on the surface of celestial bodies, such as the Moon. Unfortunately, the IAU officially does not recognize any instance of this lunar feature.

3.8. Dorsa

Lunar dorsa is the latin name for wrinkled ridges, commonly found within the confines of lunar maria. These features are low, sinuous ridges which can extend for upto several hundred kilometers (in terms of length) [14].

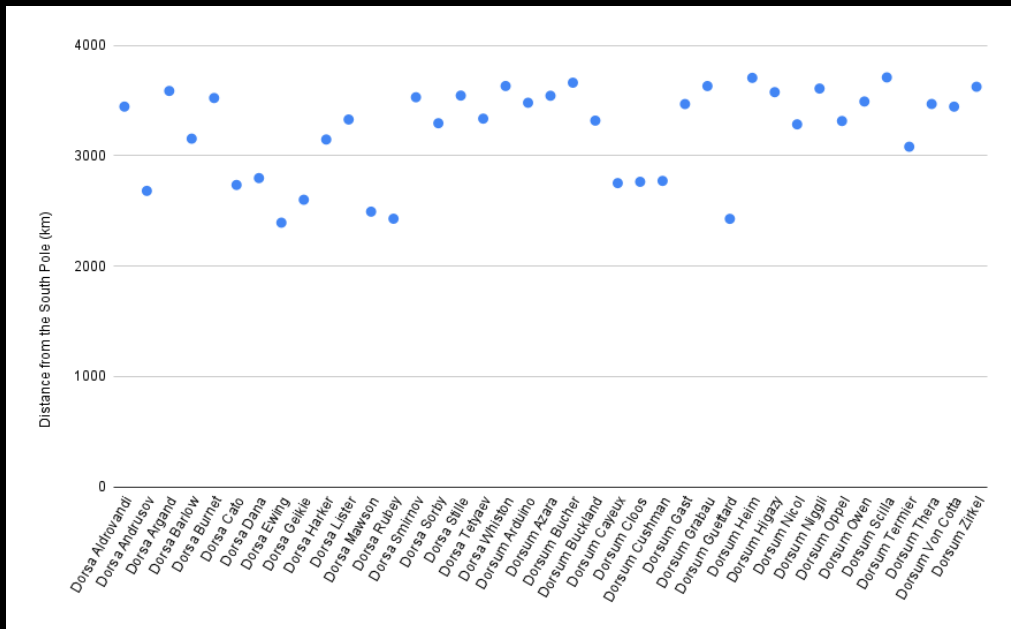


Figure 11: Scatter Plot of lunar dorsa with respect to their haversine distances from the South Pole.

Different hypotheses have been proposed which explain the formation of the lunar dorsa, yet the most widely accepted notion indicates their formation due to tectonic activity. Based on the analysis projected in Fig. 11, *Dorsa Ewing* happens to be in close proximity to the South Pole with an approximate distance of 2393.72528248236 km and diameter of 261.57 km.

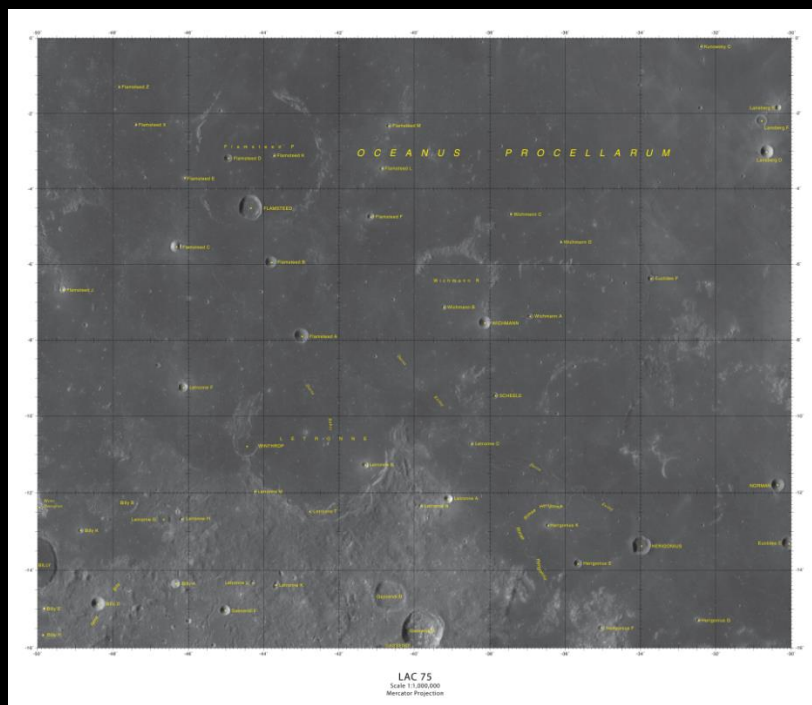


Figure 12: Lunar Quadrant with the center point of Dorsa Ewing [12].

3.9. Promontoria

As documented by the IAU, lunar promontoria refer to features which form a cape or headland on a lunar mare.

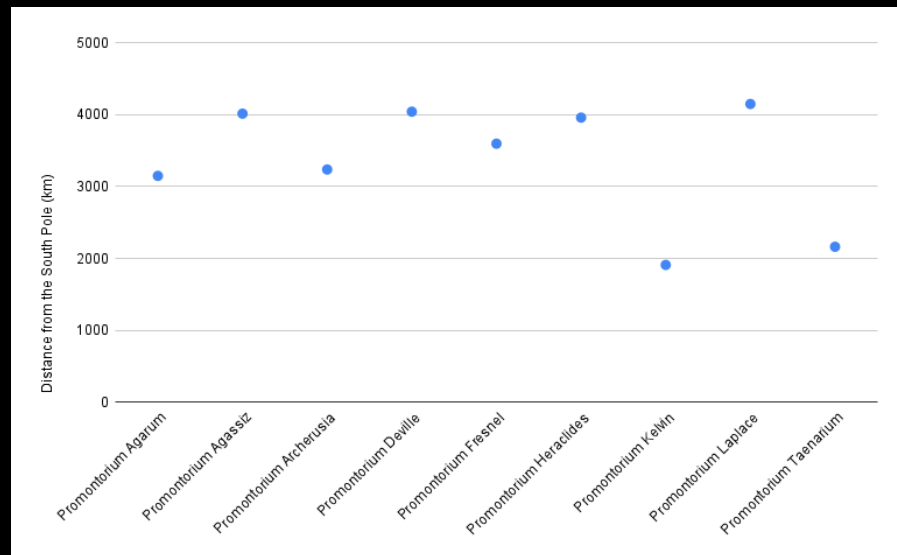


Figure 13: Scatter Plot of lunar promontoria with respect to their haversine distances from the South Pole.

A high-level comparison of the lunar promontoria suggests Promontorium Kelvin to be a potential base location, especially in terms of its proximity to the lunar south pole relative to other similar features.

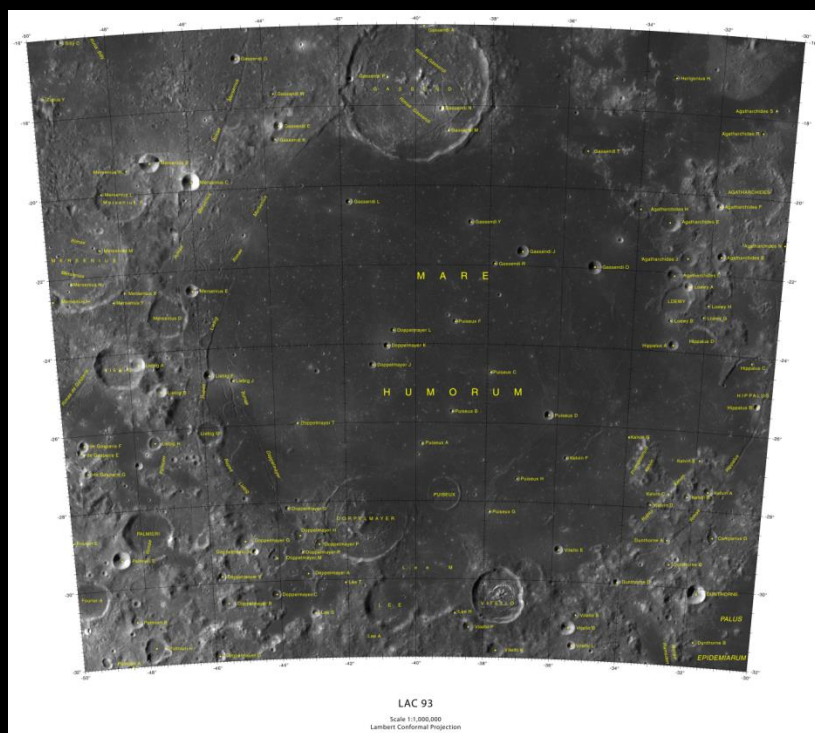


Figure 14: Lunar Quadrant with the center point of Promontorium Kelvin [12].

Promontorium Kelvin is a headland on the near-side of the Moon, located southeast of Mare Humorum and approximately 1911.8872442426248 km distant from the lunar south pole with an approximate diameter of 45.01 km.

3.10. Catanae

Catanae is the term (dervied from Latin) used to describe a chain of craters. These features constitute lines of regularly spaced impact craters, relatively the *same size and age*. They are most commonly formed as a result of a comet or asteroid with low tensile strength being pulled apart by the tidal forces of a larger astronomical body during a close pass to one another during orbit. The comet or asteroid separates into a train of fragments roughly equal in size which then proceed to collide with the surface of the larger body (usually a moon or planet), leaving a distinct trail of same aged craters that radiate out in a straight line from a single original impact site [15].

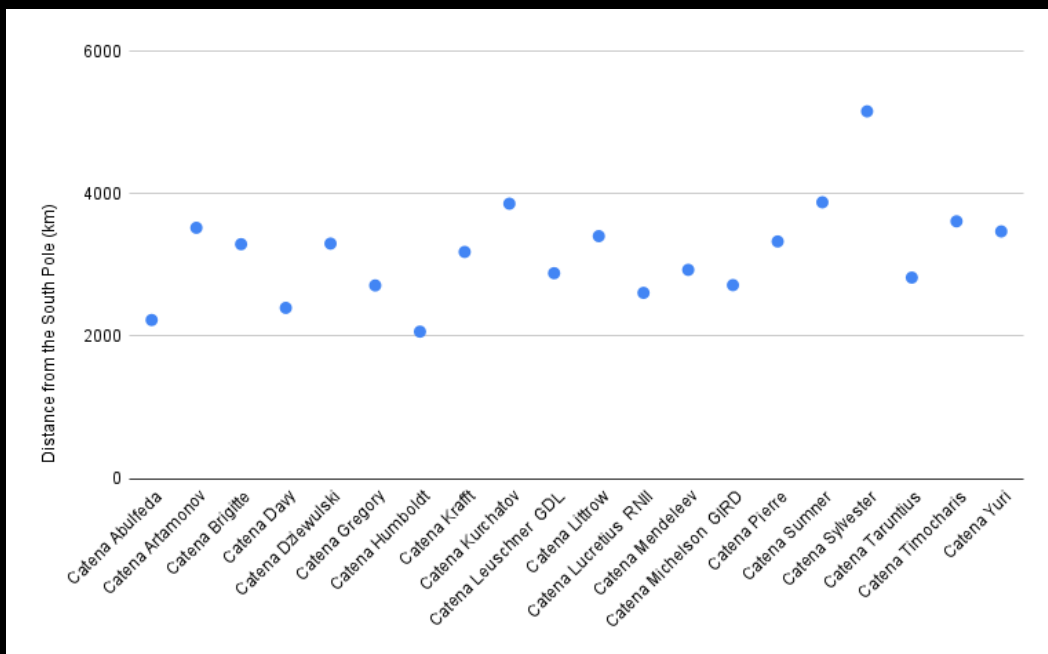


Figure 15: Scatter Plot of lunar catenae with respect to their haversine distances from the South Pole.

Yet again, the implementation of the prior analysis reveals Catena Humboldt to be the closest to the lunar south pole, at a distance of about 2062.59429585064 km.

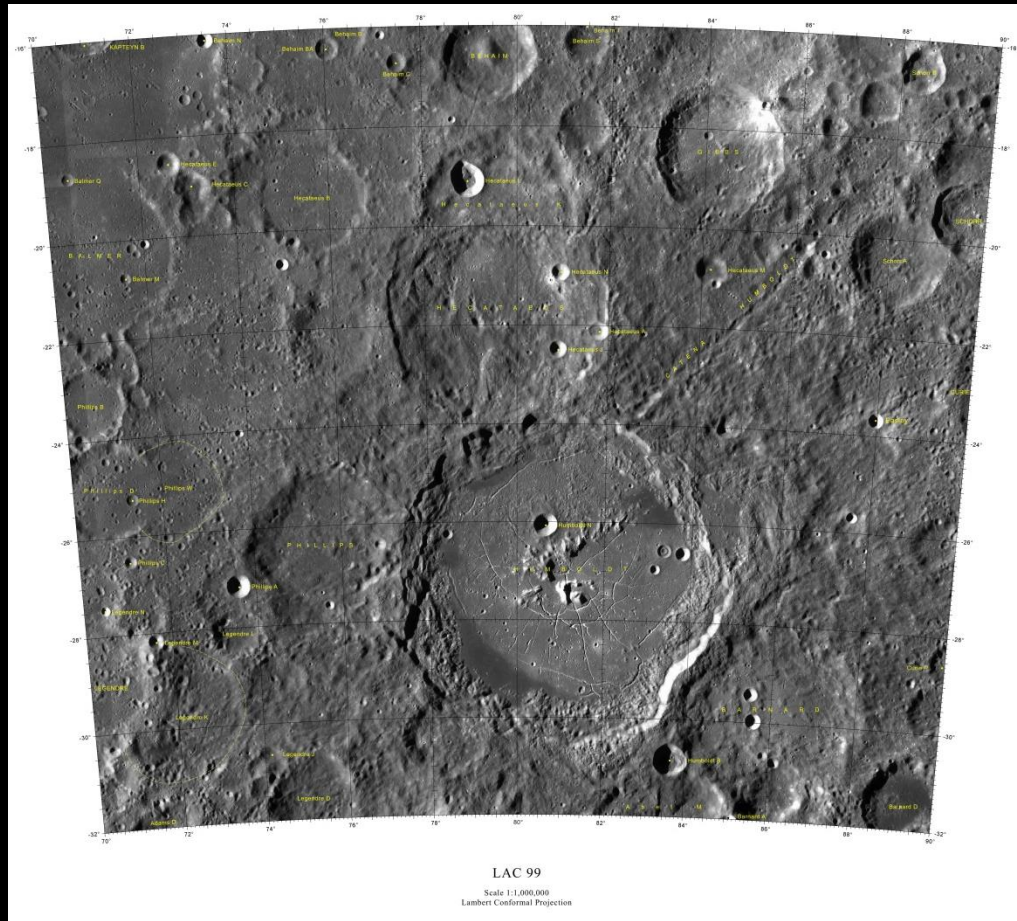


Figure 16: Lunar Quadrant with the center point of Catena Humboldt [12].

Catena Humboldt is the crater chain that extends northeast from the 189-km diameter crater Humboldt and is perhaps a potential site for a future moon base.

3.11. Oceani

Lunar oceani, according to the IAU, are defined as *very large dark areas* on the lunar surface. As per the latest documentation, only *Oceanus Procellarum*, famously known as the *Ocean of Storms*, has been officially adopted by IAU.

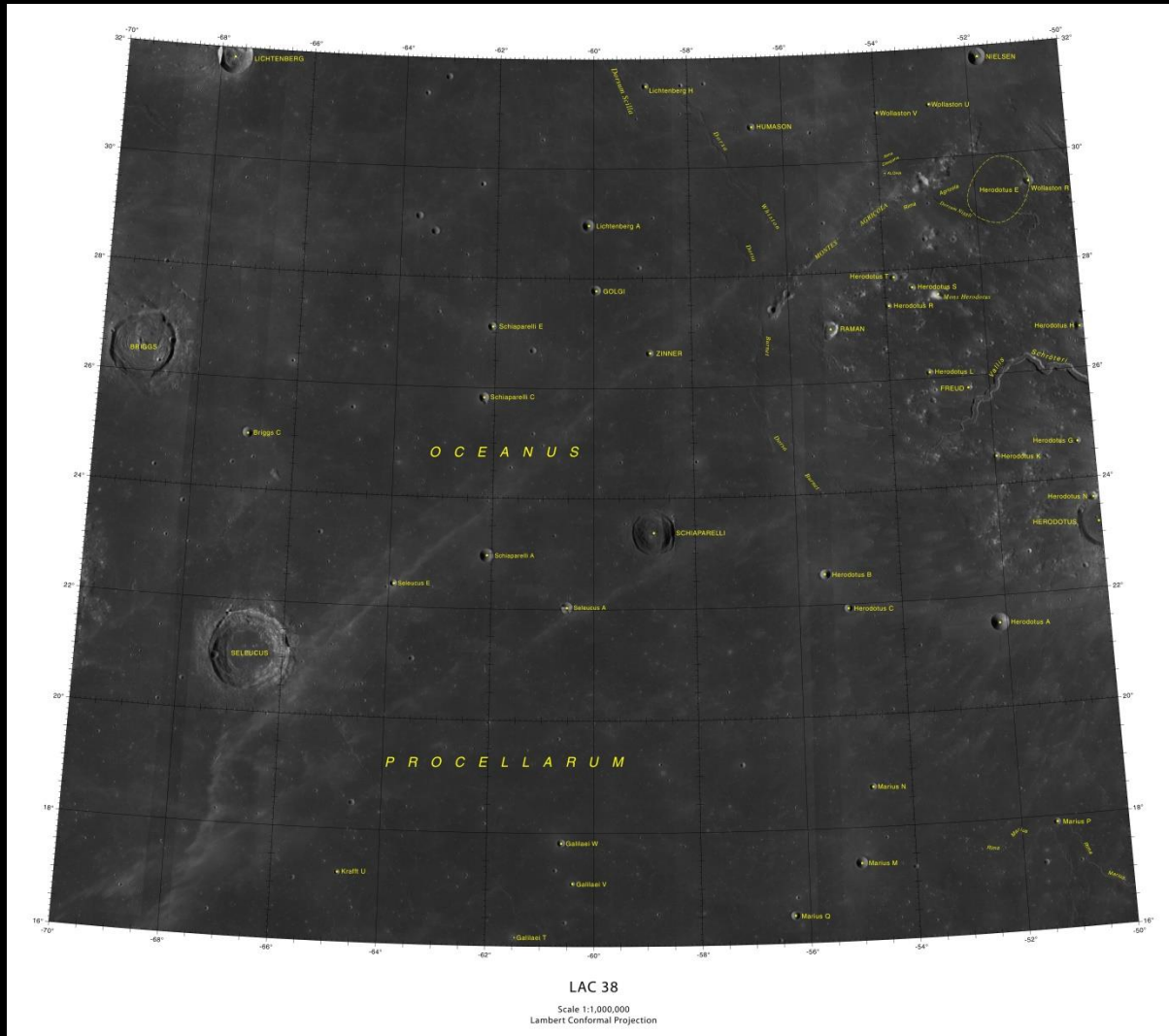


Figure 17: Lunar Quadrant with the center point of Oceanus Procellarum [12].

Oceanus Procellarum, a vast dark patch visible on the western edge of the Moon's near side, has long been a source of mystery for planetary scientists. Some have suggested that the “ocean of storms” is part of a giant basin formed by an asteroid impact early in the Moon’s history [16]. It extends over 2500 kilometres along its north-south axis and covers an area of about four million square metres. *Unlike other lunar maria, Procellarum is not contained within a single well-defined impact basin. Minor bays and seas, such as Mare Nubium and Mare Humorum (to the South), reside around its edges. To the northeast, Oceanus Procellarum is separated from Mare Imbrium by the Carpathian Mountains* [17]. Situated at an approximate distance of 3355.8851914406237 km from the lunar south pole, this feature marks the landing sites of lunar probes Surveyor 1, Surveyor 3, Luna 9, Luna 13 and the Apollo 12 mission and is thus, a notable site for further exploration.

3.12. Rimae

Lunar *Rima*, latin for rille, typically represents long narrow depressions on the surface of the moon that resemble channels. The three types of rille that have been discovered on the lunar surface include *Sinuous*, *Arcuate*, *Straight* rilles, the first being the most common feature[18]. *Formed during the eruption of basaltic lavas, the sinuous rilles may have evolved into lava tubes when segments of the channel roofed over.* Although they are of orders of magnitude larger than the terrestrial counterparts, lunar sinuous rilles and their associated lava tubes, may have remained intact since their formation millions of years ago, and thus are arguably a possibility for lunar bases [19].

Based on the data documented by the IAU and the implementation of the closest feature analysis, Rimae Janssen emerges as the rille closest with a distance of approximately 1340.292088747407 km from the lunar south pole.

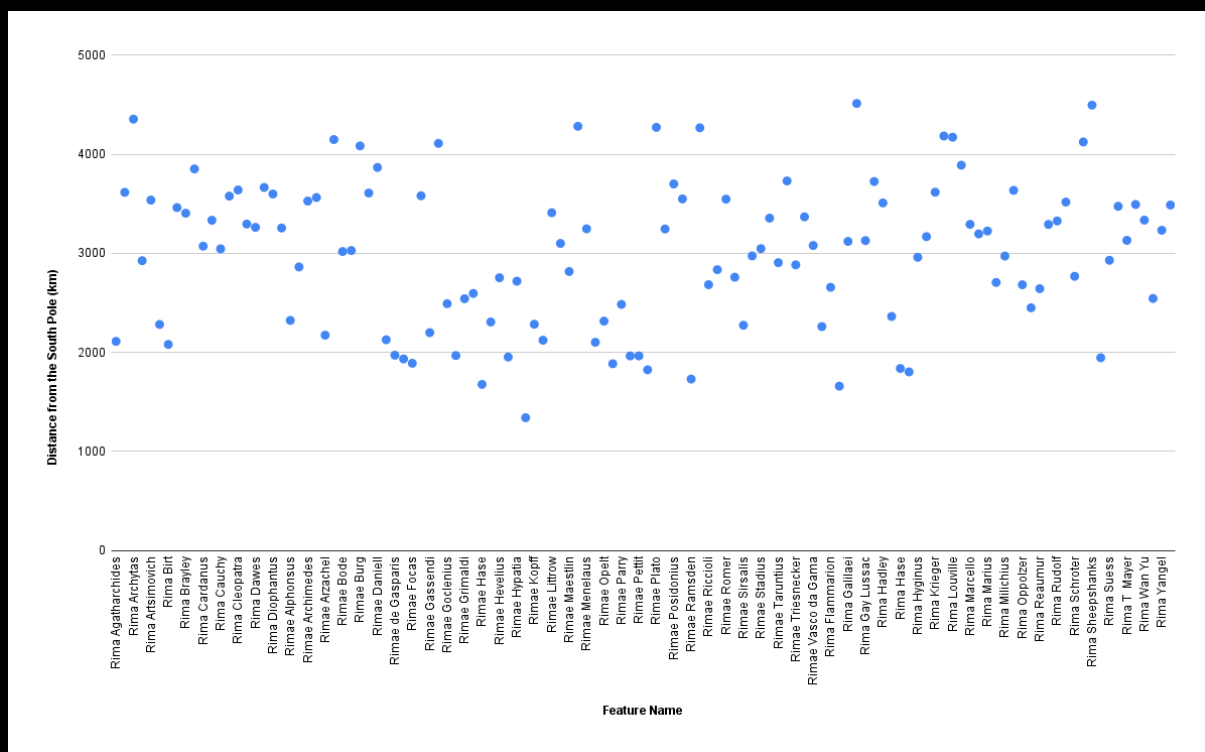


Figure 18: Scatter Plot of lunar rimae with respect to their haversine distances from the South Pole.

Rimae Janssen is a rille system that curves from the rim of Fabricius to the southeast of the outer wall of Janssen crater, extending for a distance of about 140 km.

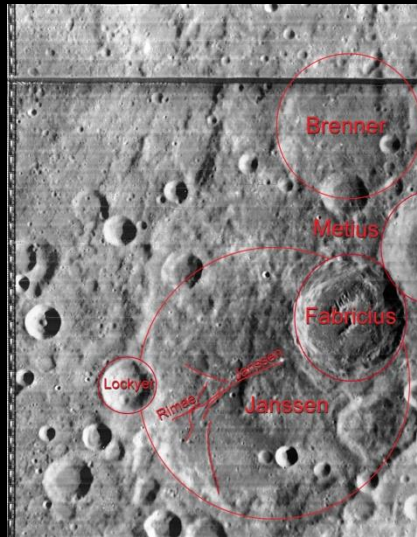


Figure 19: Rimae Janssen with Med. Res. Photo Center Coordinates $42.77^{\circ}\text{S}/37.87^{\circ}\text{E}$ [5].

3.13. Rupes

Out of the 18 different categories of lunar features recognized by the IAU, lunar rupes holds an unique position in the history of lunar geology. A Rupes is a surface manifestation of the structural faulting that formed when the lunar crust pulled apart [20].

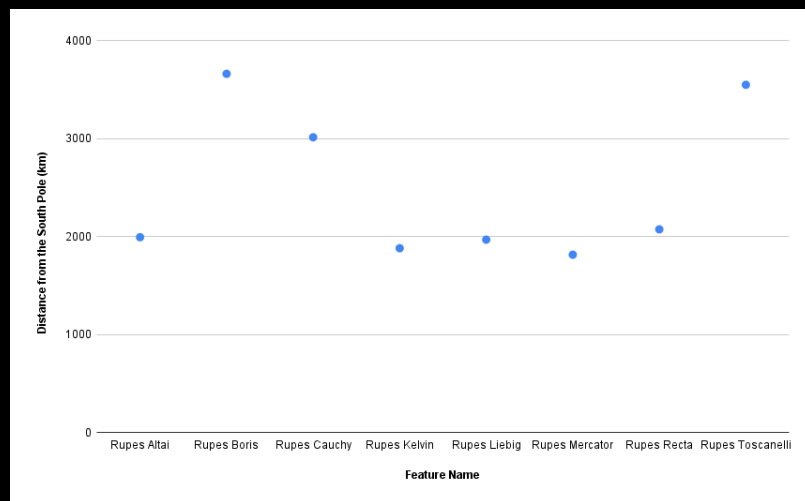


Figure 20: Scatter Plot of lunar rupes with respect to their haversine distances from the South Pole.

Based on the analysis, Rupes Mercator, which is an escarpment on the Moon and named after the nearby crater Mercator, turns out to be the closest to the

lunar south pole although further analysis is still a requisite to confirm its inclusion into the list of potential base locations.

3.7. Montes

Mons (plural: montes) are referred to mountains or mountain ranges on celestial bodies other than Earth. Lunar mons were the consequence of a variety of geological processes. Some of the largest and well-known ones are due to ancient volcanic activity while others were formed by the impact of asteroids and comets. Although apparently uninhabitable, but careful studies have revealed the potential of lunar mons for the accelerated construction of human colonies, which some characteristic features being advantageous over some of the most suited impact craters.

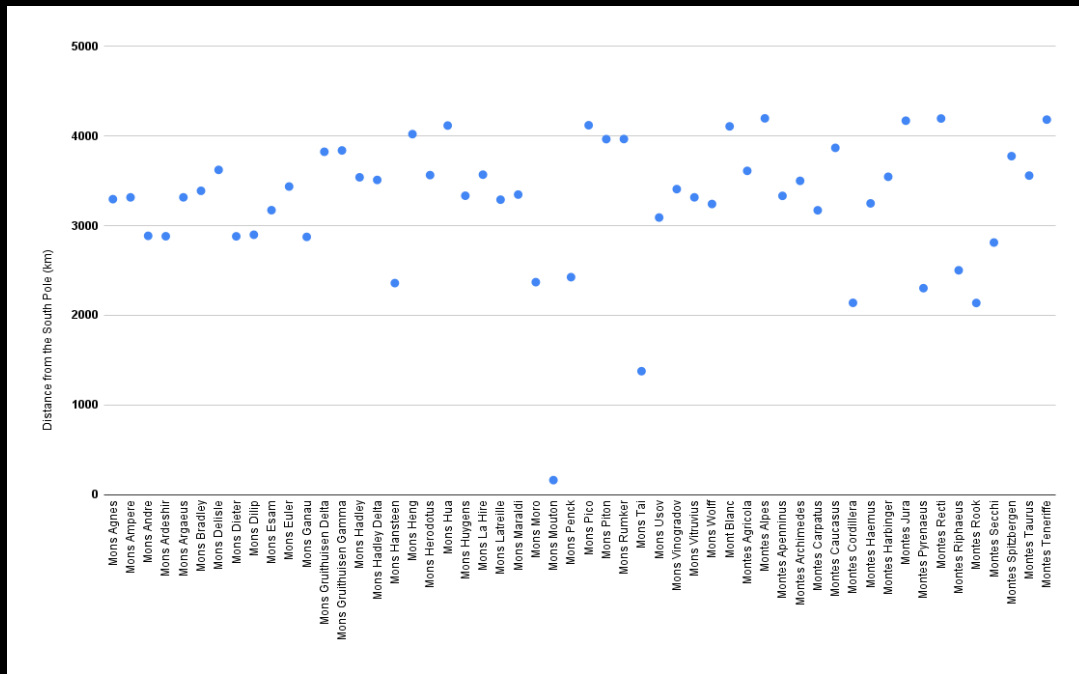


Figure 21: Scatter Plot of lunar montes with respect to their haversine distances from the South Pole.

Based on the minimum distance approach, the data put-forth by IAU [12] unveils *Mons Mouton* to be the closest to the lunar south pole, with an approximate distance of 164 km. As can be inferred from the analysis, Mons Mouton, also informally referred to as *Leibnitz Beta*, is a wide, relatively flat-topped mountain near the lunar south pole [21].

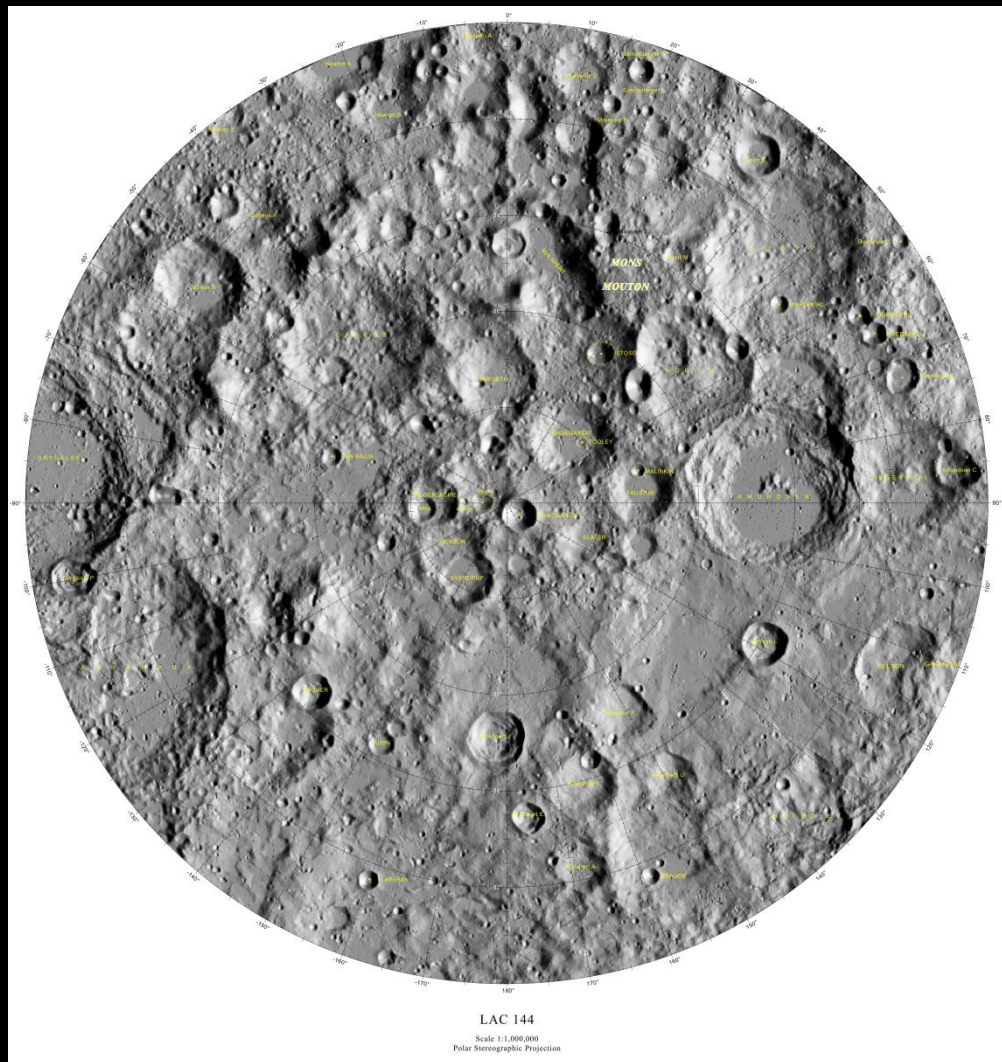


Figure 22: Lunar Quadrant with the center point of Mons Mouton [12].

According to Dr. Sarah Noble (VIPER program scientist at NASA Headquarters, Washington), this unique feature offers high sunny spots, relatively flat surface, evidence of water ice, and allowance of long stretches of direct communications with ground stations on Earth [21], thus proving to be an excellent site for future landing and state-of-the-art lunar base.

3.8. Valles

Lunar valles are referred to as lunar valleys which are long depressions on the lunar surface. Although with an upper bound on the length of this feature that attains hundreds of kilometers, lunar valles are only a few kilometers across. The origin of valles is hypothesized to be the interplay of tectonic and volcanic activity, including impact events due to the evidence of craters or rays (ejecta from impacts) that intersect them [22]. Near lunar maria, these are sometimes

referred to as *rimae* (as discussed previously) but the core aspects instrumental in their distinction are the dimension and the geologic origin of these apparently similar features on the moon.

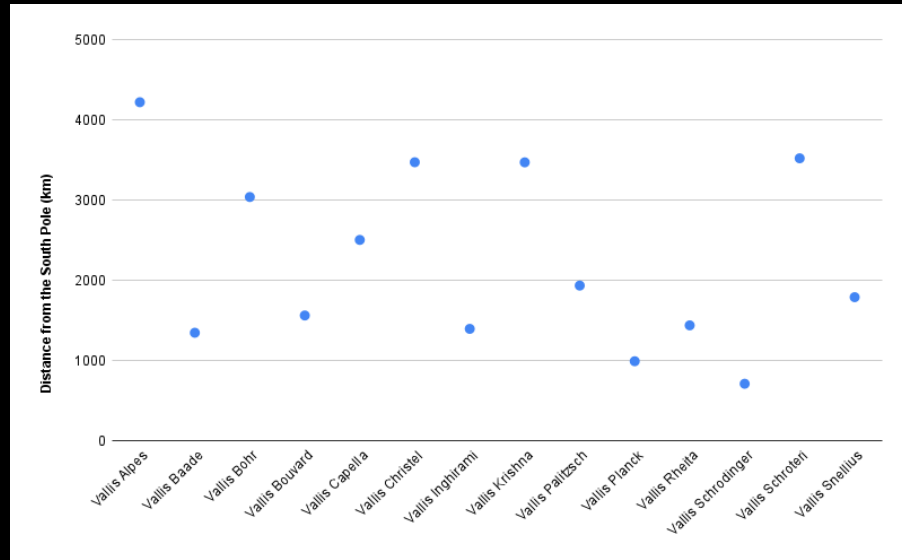


Figure 23: Scatter Plot of lunar valles with respect to their haversine distances from the South Pole.

From the prior analysis signified in Fig. 23, *Vallis Schrodinger* is at the closest distance from the lunar south pole, being in proximity to the Schrodinger crater (or basin) which in-turn is a potential landing site for future lunar missions.

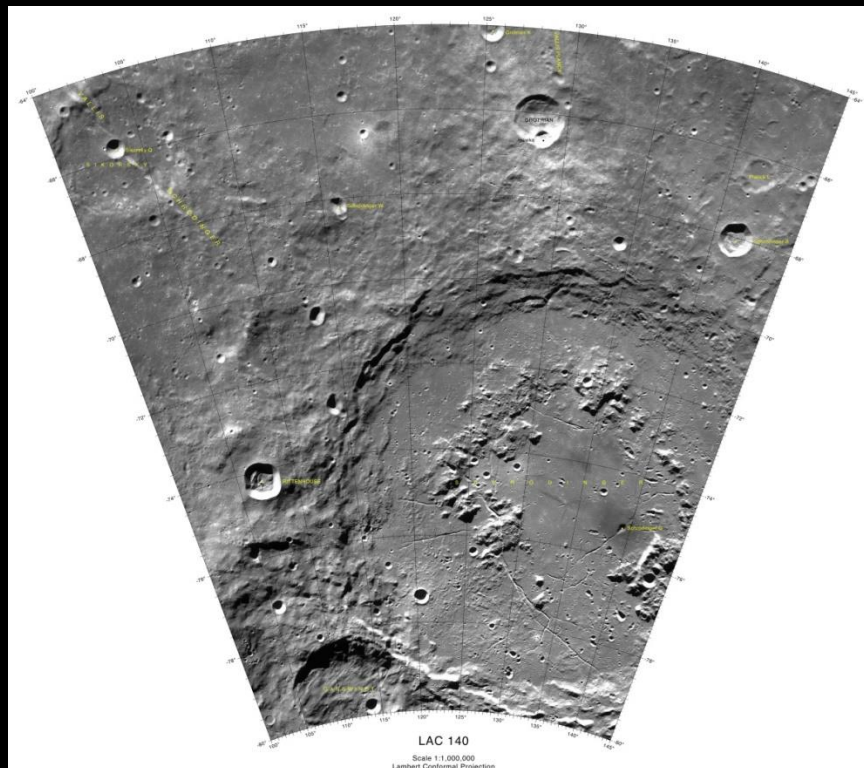


Figure 24: Lunar Quadrant with the center point of Vallis Schrodinger [12].

Vallis Schrodinger is a long, nearly linear valley that is oriented radially to the huge Schrodinger basin and was most likely formed during the original impact that created Schrödinger. The valley is shaped like a long groove in the lunar surface. It begins at the outer rampart of ejecta surrounding Schrödinger and continues to the north-northwest until it crosses the rim of the crater Moulton. About mid-way along its length it crosses the crater Sikorsky and is overlaid in turn by the small satellite crater Sikorsky Q [23].

3.10. Lunar Pits

Lunar pits were first discovered on the Moon by JAXA's SELENE spacecraft in 2009 which have since then, sparked the possibility of their exploration in profundity. Pit craters originate from the collapsed ceilings of subsurface void spaces, such as natural caves or lava tubes [24]. Although collapsed pits have been discovered on every major terrestrial body of the inner solar system, the presence of *distinct overhangs* have been found on only the Earth and Moon, which are *typically the result of a structural instability triggered by seismic activity, tectonism, and/or impacts*. There are 16 confirmed collapse pit features on the moon potentially stemming from lava tube networks and a lot more resulting from the collapse of impact melt material [24]. Pits which belong to the former class have diameters ranging between 15 to 150 m and can be discovered between latitudes of 36 degrees S to 45 degrees N, thus enabling direct communications to Earth (being mostly on the near side of the Moon). The pits, and in turn, the caves that these might lead to would offer organic protection from solar radiation, cosmic rays and micrometeorites, thus making them some of the best sites for future lunar settlements.

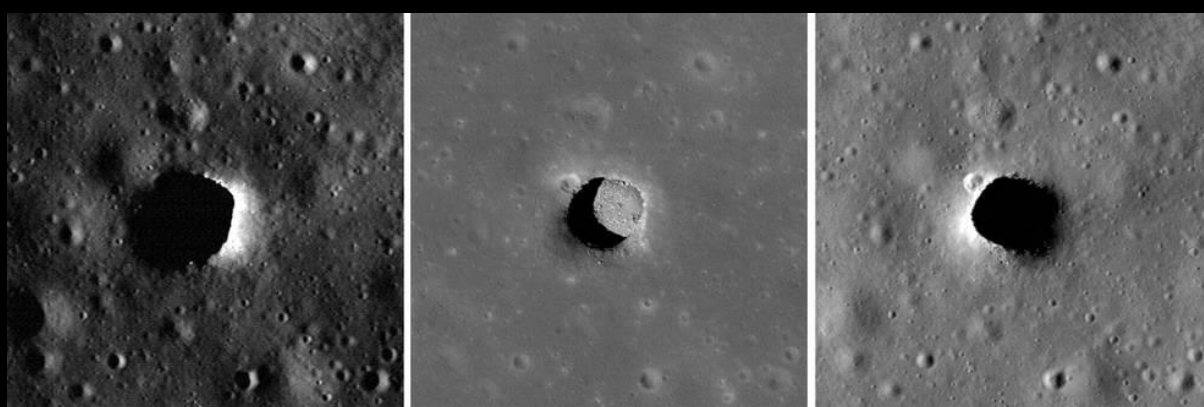


Figure 25: Marius Hills pit captured by LRO at three different times [24].

Recent results, based on the analysis of pits situated in Mare Tranquillitatis and Mare Ingenii, reveal that thermal environments within the pits and inside the caves are *moderated substantially more than the surface*. Furthermore, the cave temperatures have been formulated to be nearly constant and isothermal at about 290 K, and this approximation holds *if the surface area internal to the cave is large, compared to that of the pit through which radiation enters and exits.*

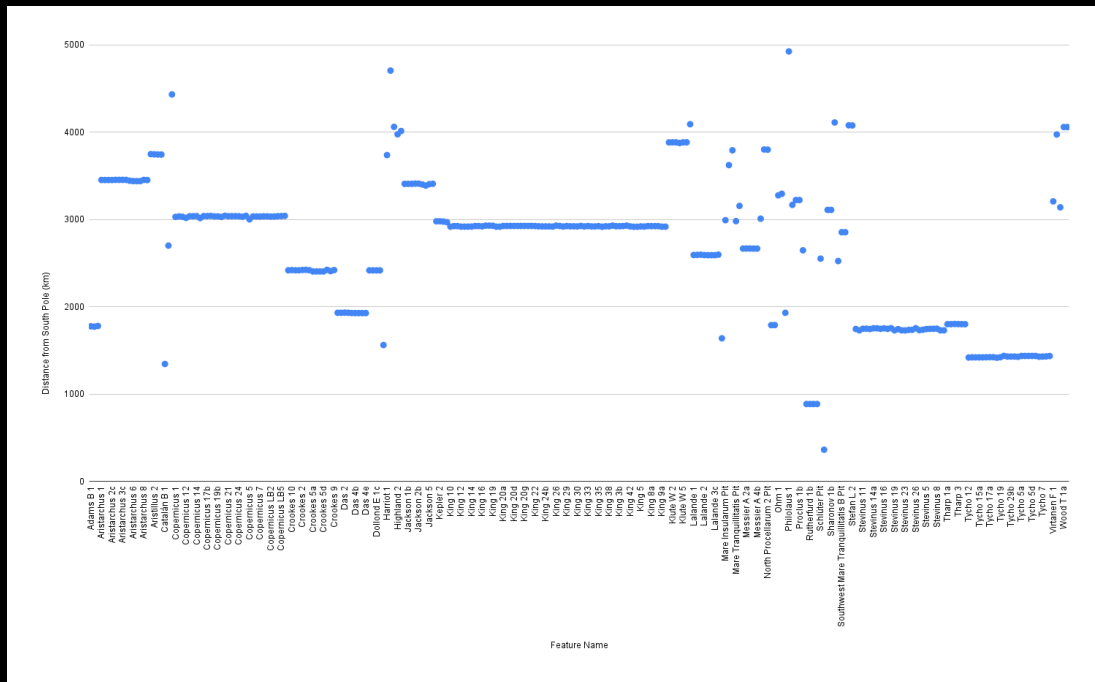


Figure 26: Scatter Plot of lunar pits with respect to their haversine distances from the South Pole.

Appertaining to the extensive data on lunar pits published by the Arizona State University [28], the haversine distances of the instance features based on their center coordinates (as reflected by Fig. 26) leads to choosing *Schomberger A 1* as the closest site, with Schomberger A as the host feature.

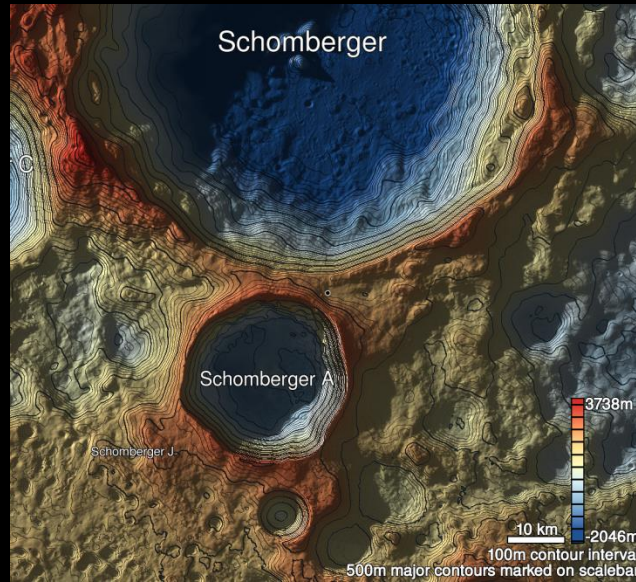


Figure 27: Schomberger A 1 Shaded Relief , LROC [28].

Schomberger A 1 is a lunar pit which belongs to the latter class, with its terrain originated from the collapse of impact melt. But, the feature has a very large boulder in the middle (about 3m wide visible) and that occupies much of the pit's interior [28]. This calls for a more feasible site to be analyzed in terms of all the factors that govern the choice of ideal lunar bases. In light of the next closest instances, the 4 lunar pits housed within the host feature Rutherford crater turn out to be the viable sites for exploration.

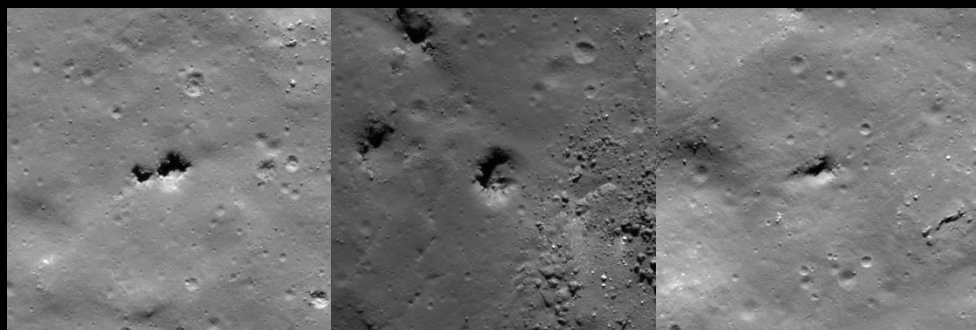


Figure 28: Rutherford 1a, 1b, 2 and 3 (from left to right) [28].

Since their approximate distances from the lunar south pole are roughly equal (i.e. 886 km), we must analyze every pit crater and discuss the potential merits and limitations associated with the same.

Table 1: Dimensions of the chosen pit craters [28].

Name	Depth	Inner Pit Diameter	Funnel Diameter
Rutherford 1a	5m	14m x 13m	18m x 17m

Rutherford 1b	> 3m	9m x NAm	15m x 14m
Rutherford 2	9m	24m x 19m	36m x 30m
Rutherford 3	3m	18m x 8m	31m x 18m

Rutherford 1a, an impact melt pit, is the larger one of a pair of pit craters. Roughly square in shape and with walls oriented about 45 degrees away from a line drawn through the pair of pits, the feature has a clear floor and appears to have a slope running from south corner to floor which maybe traversable. In contrast, Rutherford 1b is also perhaps an impact melt pit (smaller of the pair) but the ambiguity of data makes further deliberations uncertain. Rutherford 2, also an impact melt pit, is round with east wall sloping down to the floor, with the existence of an entrance ramp. Furthermore, there exists a nearly 200m long, 35m wide, and 7m deep linear depression running NW/SE starting about 60m to the NW, and a few more round to elliptical depressions with some degree of vertical wall/rim outcropping running in a chain about 50m south of that [28]. Rutherford 3, unlike others, is an collapsed uncertain impact melt pit with its only vertical wall being the one to the north and others being slopes [28].

In order to analyze and pinpoint the most suitable sites in case of a multitude of options, we need to delve deeper and consider the critical factors instrumental in determination of the potential base locations. One such inevitable criterion is the potential of ISRU (In-Situ Resource Utilization) of which the presence of lunar water ice and other volatiles is a major aspect. Since the host feature, crater Rutherford, is itself a sub-feature of the larger crater Clavius and that the latter has been proven to constitute ‘lunar water’ in voids between the regolith particles of the soil by NASA’s SOFIA telescope (conc. 100-400 ppm estimated) [29, 30], the very existence of hydration and the significant implications for sustained future lunar exploration enhances the importance of Rutherford pit craters to be investigated in profundity.

3.6. Basins

Impact basins are primary geological structures and their formation is a fundamental process in the evolution of the Moon [7, 8]. Yet not disregarding the inconsistency in basin identificaton due to the implementation of various standards [9], we consider basins to be craters that have a diameter of more than or equal to 300 km [26], in accordance with the commonly stated convention.

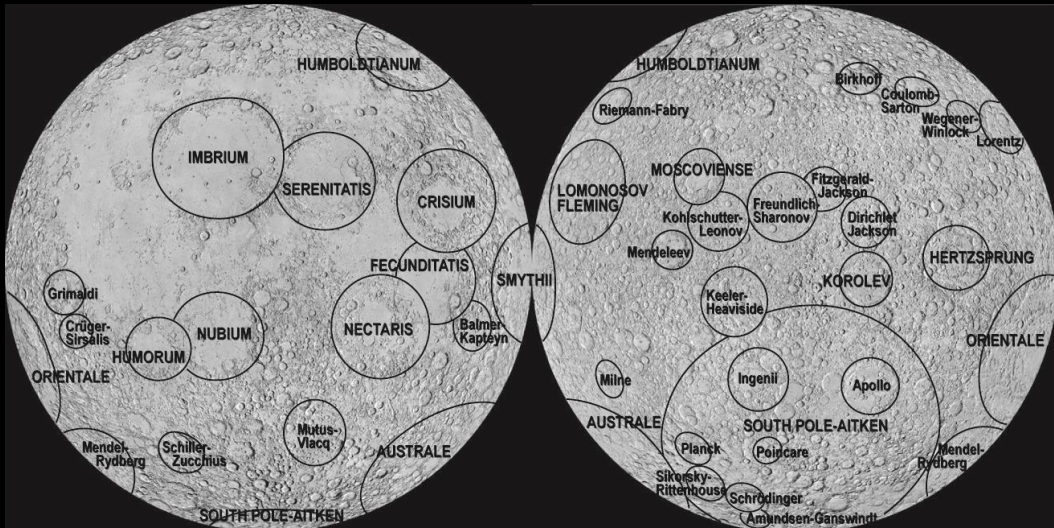


Figure 26: A map of the moon's major impact basins on the near side (left) and far side (right) [10].

Basins control much of the lunar geology, an instance of which are mare basalts that are mainly confined in the topographic depressions produced at the centers of these basins [11]. Therefore, analysis of lunar basins forms the basis of our search for potential base locations, while not ignoring the fact that many of these basins house other lunar features within them.

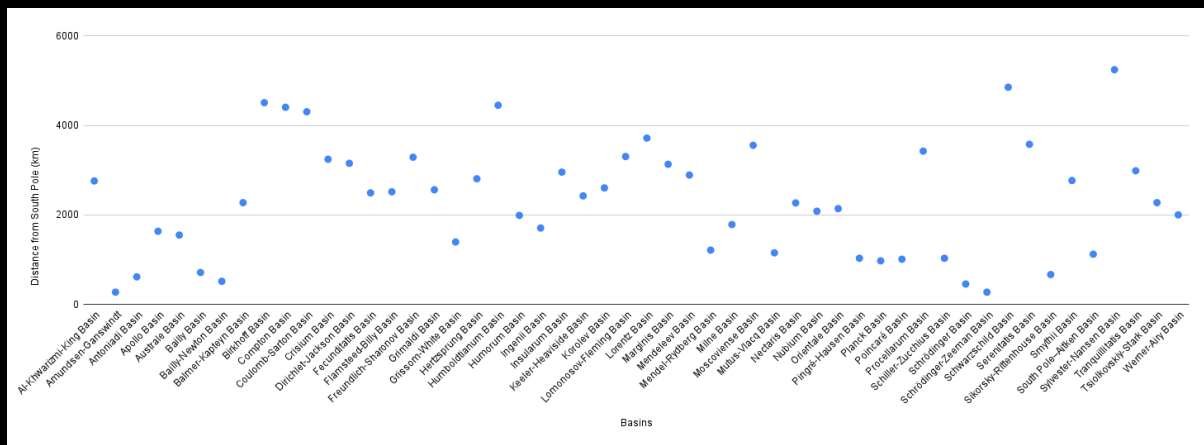


Figure 27: Scatterplot of lunar impact basins w.r.t. their haversine distances from the south pole.

Unlike the analysis performed for the former lunar features, a search for the ideal basins in the light of the least distances from the south pole might result into a misinterpretation of the results, owing to the fact that many of these basins are in fact subsets of even larger basins. In line with the haversine distances from the lunar south pole, three basins emerge to be the closest,

namely, the Amundsen-Ganswindt, Antoniadi, and Schrodinger-Zeeman, with an approximate distance of 273 km based on their center coordinates.

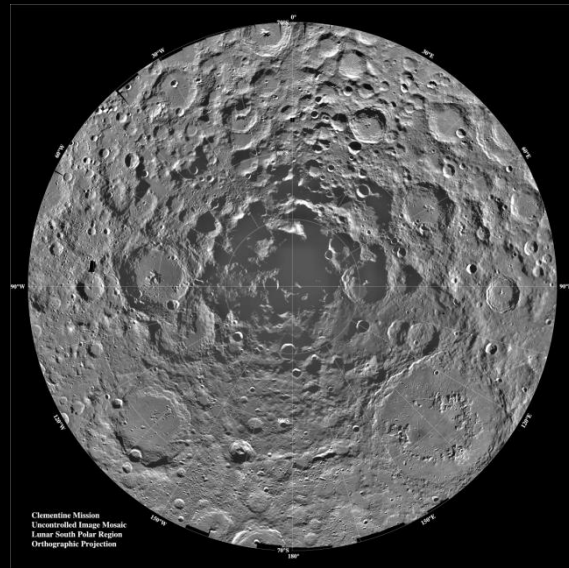


Figure 28: Lunar mosaic of ~1500 Clementine images of the south polar region of the moon representative of the three basins [27].

At this point, a computational misinterpretation of the best locations might come up in light of the fact that the South Pole Aitken Basin (SPAB), which is the longest, oldest and deepest on the lunar surface, is at an approximate distance of 1121 km, based on the center coordinates. But in reality, the three aforementioned basins are themselves located within the SPAB! Therefore, a further qualitative analysis leads to a clear revelation that *South Pole Aitken Basin* is one of the prime targets in terms of the very first establishment of lunar research facilities, which has also been a site of immense consideration by international space agencies.

Amundsen-Ganswindt basin, the area situated between the two impact craters, spans across an estimated diameter of 335 km. Due to its proximity to the lunar south pole which is our primary factor, there may possibly exist cold traps within the basin where low temperatures may harbor water ice and other lunar volatiles and be stable as permafrost within the upper layers of the regolith. In addition, preliminary analysis of the Moon Mineralogy Mapper (M3) data has indeed revealed the presence of hydroxyl spectral signatures in areas within the basin, as shown in Fig. 29 [31], thus lighting up the possibilities for ISRU.



Figure 29: OH spectral signatures in A, B, C, D1 and E [31].

Antoniadi Basin, with a diameter of about 135 km [33] is located within the SPAB and lies between the craters Minneart and Numerov. Antoniadi's morphology makes it fall between the category of craters and multi-ringed basins, especially due to the fact that it constitutes a central peak as well as an inner ring of peaks. In fact, the deepest point on the lunar surface (i.e. -9.12 km) [33] has been pinpointed within the basin itself! The floor of Antoniadi contains geologic materials from the deepest part of SPAB, and the Moon; there is a great possibility that the impact that formed Antoniadi excavated materials from the lower crust/upper mantle. Antoniadi also displays a large number of secondary craters on its ejecta blanket. Antoniadi is therefore, a special site for research and deeper understanding in terms of its ejecta and geologic history with respect to the history of the SPAB [32].

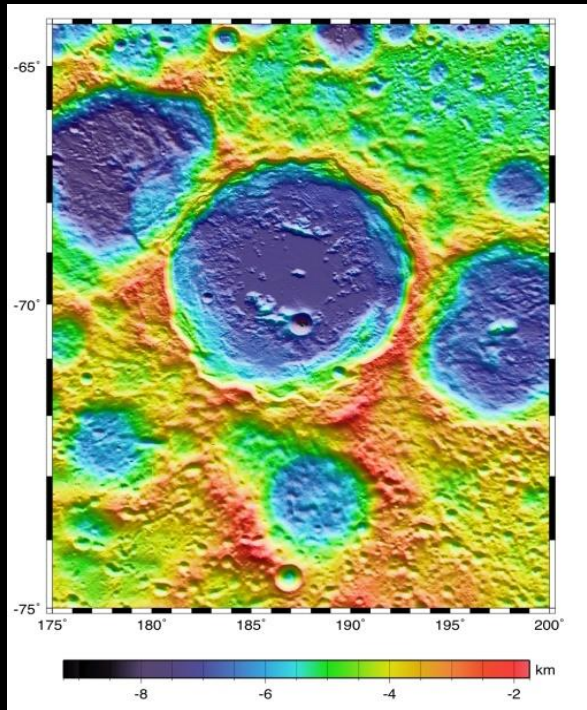


Figure 30: Antoniadi Basin based on LOLA's topographic data [33].

The Schrodinger-Zeeman basin is located on the farside between the basins Schrodinger and Zeeman and is centered on (81°S, 165°W). Based on most recent data from Chuck Wood's lunar impact basins database [34], the proposal of this basin has been relatively new and further research of this feature is yet to be done. The basin has a double-ring structure, with an inner ring diameter of 150 and an outer-ring diameter of 250 km. The concentric rings are well preserved and the overall geology of the basin makes it a potential candidate for a lunar base.

3.7. Revisiting Craters:

Alongside the rigorous analysis which led to the rediscovery of some of the best zones for sustained habitation on the lunar surface, we henceforth focus on most abundant geological feature on the moon, craters. Despite the fact that craters were the very first feature introduced in this report, yet the vast majority of lunar craters calls for the inclusion of additional criterion to filter out the first set of feature instances that could in turn, lead to the detection of the best locations from within the immense diversity of impact craters.

The proximity to the south pole, being the basis for the entirety of our analysis, we therefore choose the secondary conditional for craters in the form

of a threshold distance, which would be selected based on the haversine distances of candidate sites analyzed previously with respect to the south pole. In light of the approximate distances of the 17 different categories of lunar geology, the roughly equal haversine distance of the three candidate basins, i.e. 273 km, serves as the upper bound for the survey of craters, owing to the fact that the locations which are at a distance of less than that of the assigned threshold would, of course, be a clear win over the other feature instances, not as well ignoring the crucial aspect of ISRU associated to each of the candidate locations.

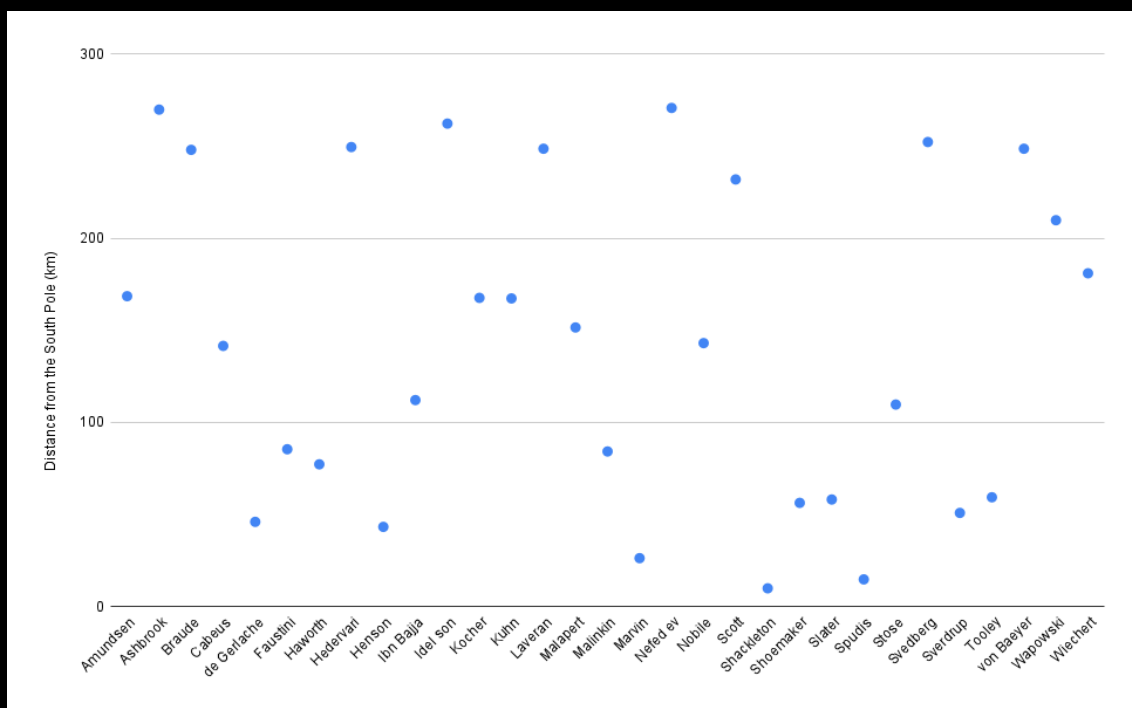


Figure 31: Impact craters with haversine distance less than the upper bound.

This shift in the course of our analysis has indeed proven to be beneficial, primarily due to the reduction of the targets to only 31 candidate spots.

Starting off, we propose the classification of lunar zones, depending upon the approximate distances of the 31 craters from the lunar south pole — the **Primary Zone**, which includes sites with haversine distances less than or equal to 100 km, **Secondary Zone**, which incorporates sites at a distance ranging between 100 and 200 km, and the **Tertiary Zone**, which includes sites which are at an approximate distance of more than 200 km. We shall explore every possible location and discuss the advantages and trade-offs related to the construction of the first human bases in the chosen sites.

3.7.1. Primary Zone

The *Primary Zone* comprises 12 impact craters, with each instance being of prime interest due to their greater proximity to the lunar south pole.

Table 2: Craters belonging to the Primary Zone.

Feature Name	Distance from South Pole (km)
Shackleton	10.0067056399692
Spudis	14.8584417078331
Marvin	26.38131486901
Henson	43.3623911065339
De Gerlache	46.0914926447071
Sverdrup	50.9432287125716
Shoemaker	56.401431788918
Slater	58.220832814367
Tooley	59.4337668313328
Haworth	77.324543581581
Malinkin	84.2989141791357
Faustini	85.5118481961013

The Shackleton crater is the closest one to the lunar south pole (in fact, nearly coincident) and is thus, one of the top candidates for the first human bases on the moon. While the peaks along the crater's rim are exposed to continual sunlight, its interior is a PSR, which in turn, sparks the precious possibility of the existence of lunar water ice and other volatiles. Furthermore, the exploration of Shackleton's interior shall enable extensive research towards unveiling the timeline of lunar environment over long periods of time [35].

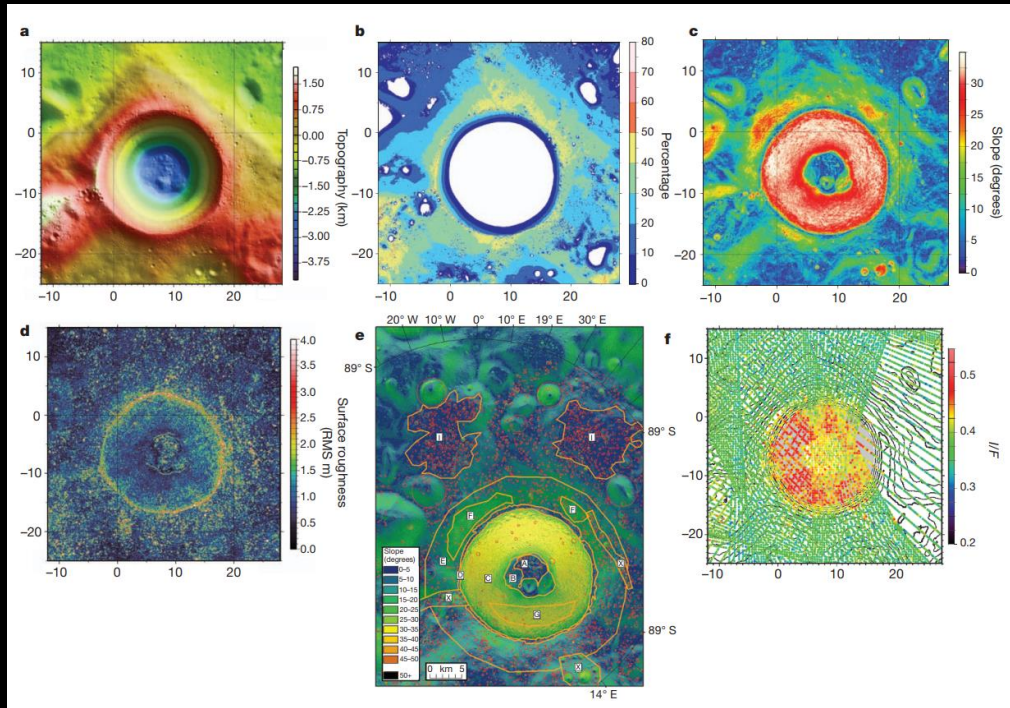


Figure 32: Detailed characterization of the Shackleton Crater [36].

The topography reveals the near-axisymmetric bowl-shaped nature of the crater, in which the crater rim and interior walls are well preserved. The slope profiling indicates that slopes are greater in the mid-levels of walls. At a wavelength of 1,064 nm, the floor of Shackleton crater is darker than its interior walls, but both floors and walls are considerably brighter than the surrounding terrain, including the interiors of nearby craters that are both shadowed and sunlit. This relative brightness of the floor surfaces the possibility of the deposition of volatiles. The measured reflectance of the floor can be explained by a micrometre thick surface layer of 22% ice mixed with rock, with a possibility of greater ice contents distributed throughout a thicker layer but cannot be constrained from LOLA's reflectivity measurement [36]. Although additional insights from the LRO Mini-RF orbital radar, with the conjunction of observational inferences, are suggestive of different explanations, yet there is strong existence for ice on both the crater's floor and walls [37].

Spudis is a 13 km wide crater located next to the Shackleton crater and is believed to be a likely destination for future lunar missions. On the other hand, the crater Marvin, whose rim is approximately 16 miles from the South pole and is next to the Spudis crater, has also been projected to be the site of exploration by Artemis III astronauts.

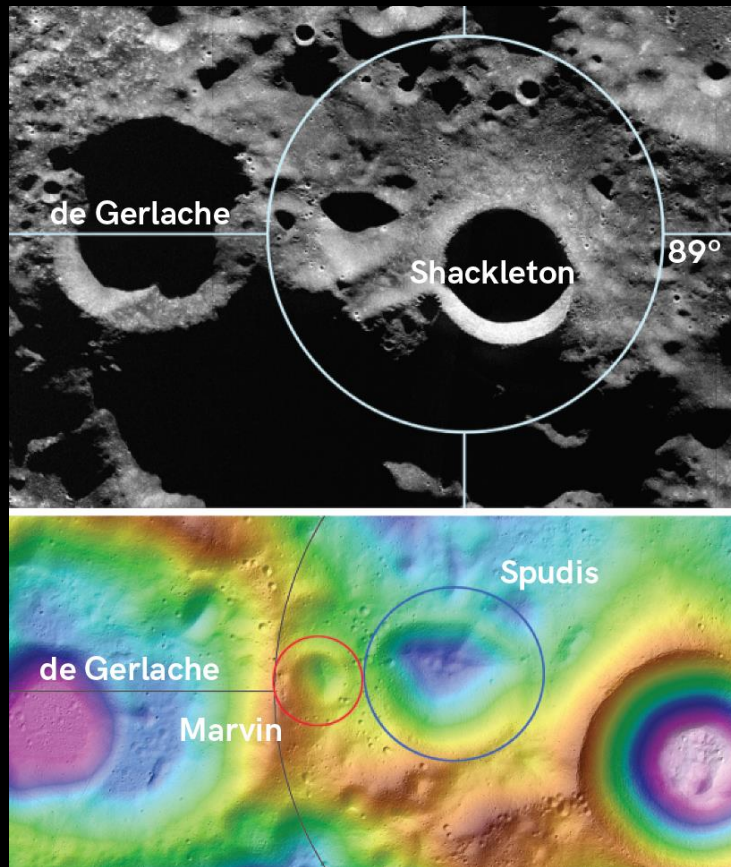


Figure 33: Location of the Spudis and Marvin craters [38].

Henson is a 43 km diameter crater located in the lunar south pole and is arguably the oldest impact crater in the south polar region. *The crater contains a PSR that may harbor ice which can be utilized to study the evolution of volatiles in the inner Solar System and for sustainable exploration of the Moon. Model calculations suggest the existence of water ice on the floor of the crater. Water ice at the surface has been detected in several locations from orbit. The floor of the crater is so cold that portions of it may also be covered with dry ice. A recent study identified several sites within the crater that are accessible with a rover [39]. Furthermore, the crater lies within the Artemis exploration zone, and thus is a prime target for future lunar bases.*

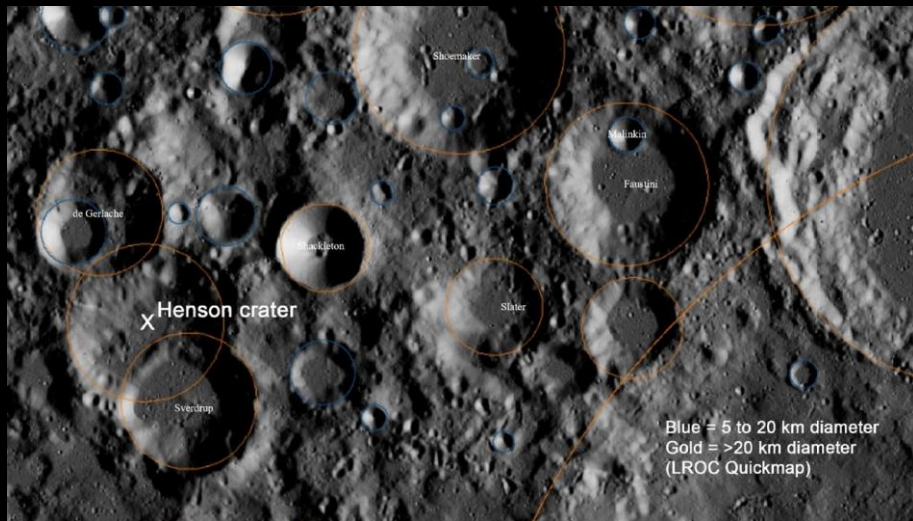


Figure 34: Location of Henson Crater w.r.t. nearby craters in the South Pole [39].

The De Gerlache crater, located just next to the crater Marvin, has been of strategic importance (even for the Artemis III Science team), especially due to the presence of an extensive PSR at its center which in turn marks the possible existence of water ice and other lunar volatiles critical for sustained stay and in-depth research of the lunar geology. In greater detail, the crater may be covered by surface water ice on 2.3% of the surface, *though the water ice may only be present as grains in the regolith* [40]. Besides, De Gerlache is in proximity to other PSR regions that are of strong interest, as well as the most illuminated zones on the lunar surface. Furthermore, the slope surrounding the PSR of the crater is shallow compared to its peers like Shackleton, thus adding up to the feasibility of robotic exploration of the region. Lastly, the highly illuminated points on the crater's rim enable the *installation of solar powerplants and associated infrastructure to support future lunar habitation* [40].

The craters Sverdrup, Shoemaker, Haworth and Faustini are four of the largest craters in the lunar south pole containing the highest concentrations of surface water-ice exposures and relatively flat floors for safe landing. The Sverdrup crater has multiple promising locations, with regions of spatially dense ice exposures (LAMP detections consistent with 0.1-2 wt%), with a potential depth of 1 m. There are 6 ice exposures located on fairly smooth surfaces, with a roughness value of ≤ 0.4 m [41]. In addition, the location is not too far from the PSR edge and crater rim (< 5 km) allows relatively easy access from a crew stationed on the rim, thus providing the greater opportunity of ISRU.

The Shoemaker crater exhibits an intact rim with numerous 1 to 10 km superimposed craters. With the ejecta blanket totally subdued, this crater is more degraded than the adjacent craters Faustini and Shackleton, but less degraded than several unnamed craters of similar size in the region [42]. Inferences from the Goldstone radar Digital Elevation Model (DEM) reveal an approximate depth of 3 to 4 km below the datum and a calculated rim height of 1.1 km above the original surface. The illuminated portion of the floor is flat and partially smooth, with scattered impact craters. The crater is simple in plan, with no evidence of a central peak [42]. Yet the floor of Shoemaker crater is one of the areas in which radar observations showed no evidence for ice. Radar beams with wavelengths of 2.5, 12.6, and 70 cm have returned echoes that are typical of highland terrain, without the strong echoes attributable to ice (there is no imaging data for the PSR region inside the crater, and therefore no conclusions can be drawn). But despite all the odds, *Shoemaker is unique due to the fact that half of the floor has been imaged by radar. The physical properties of the floor material can be modeled. This target is known to be flat, providing simple geometry for understanding impact dynamics and the ejecta plume* [42].

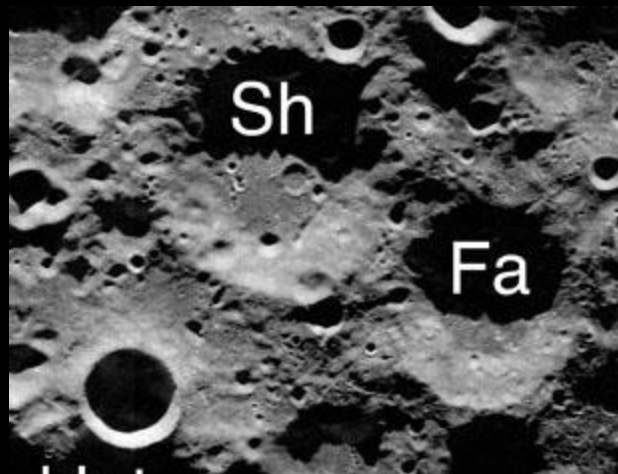


Figure 35: Shoemaker crater depicted by ‘Sh’ (Source: Wikipedia).

Crater Slater is a 25-kilometer diameter crater near the Moon’s south pole that contains a moderately sized permanently shaded region at its base. Within the shadowed portion is a bright region around a smaller, 1-kilometer diameter crater. According to Dr. Randy Galdstone, an Institute Scientist in Southwest Research Institute’s Space Science and Engineering Division [43], this small crater is likely to be extremely young and thus is of special interest for exploration.

Tooley is a 7 km impact crater situated within the permanently shadowed region of Shoemaker crater near the lunar south pole. Yet, in order to reach a valid conclusion, a deeper analysis based on still unknown data is a requisite.

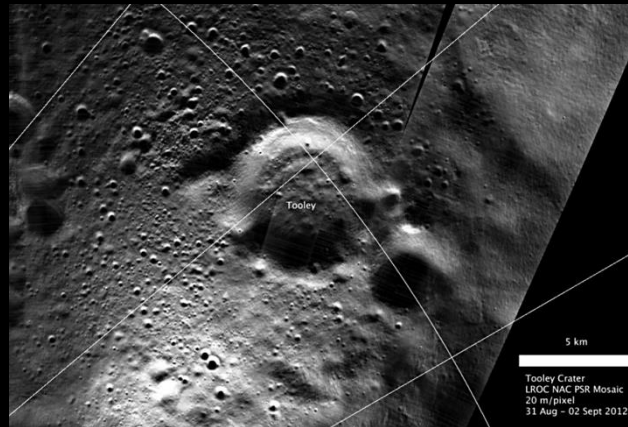


Figure 36: A mosaic of high resolution of images from the Lunar LROC's Narrow Angle Camera in a high gain mode that relies on the reflected light from nearby crater rims [44].

The Haworth crater, is yet another impact crater located at the lunar south pole, with large portions of it designated as PSRs. *For some large areas in Haworth crater, maximum temperatures never appear to exceed ~40K. This is also the region with the lowest temperature range, indicating a persistantly stable thermal regime* [45].

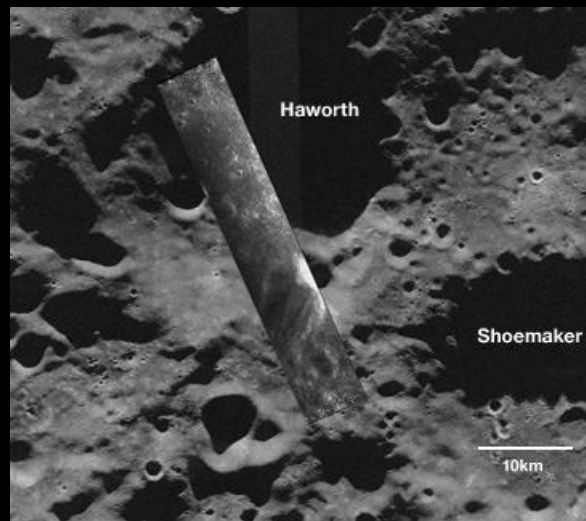


Figure 37: A Mini-RF synthetic aperture radar (SAR) strip overlain on an Earth-based, Arecibo Observatory radar telescope image [46].

Similar to the crater Tooley, Malinkin is an 8.28 km diameter crater housed within the the permanently shadowed region of the relatively larger crater Faustini.

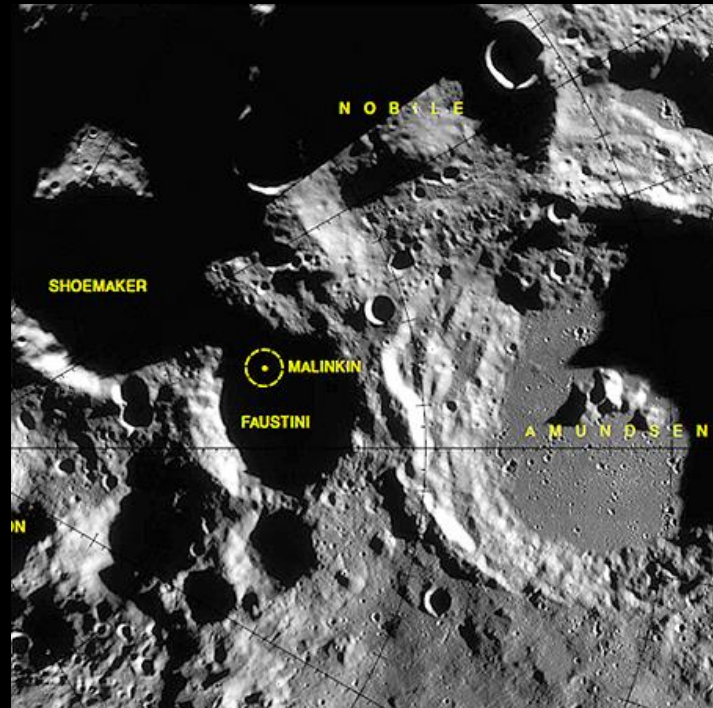


Figure 38: Location of the Malinkin and Faustini craters [47].

Faustini is a 41 km diameter, flat-floored crater located in the south circumpolar highlands. The crater has one of the highest potentials for water ice residing within its resource rich PSRs, with albedo observations suggesting water-ice content to be ~100 nm thick, estimated to range from 1-10% of the areal coverage being detected [48]. With likely evidences of lunar geological processes like impact cratering and tectonism, it is somewhat evident that this last crater in our list of primary zonal craters is likely to be a target site for future Artemis missions, which is indeed a true fact!

3.7.2. Secondary and Tertiary Zones

For the purpose of this documentation, the intricate details of the Secondary and Tertiary Zonal features are being bypassed but shall be covered in successive updates.

4. Base Locations

In light of the analysis of the 18 different instances of past lunar geological activity, there is an increased level of difficulty involved with the search of base locations, especially due to the critical aspect of every feature being unique in terms of location and geological significance, in addition to the fact that every instance possesses advantages as well as trade-offs over the others. Although this might be resolved to a large extent depending upon the extent of mission planning and the application of the state-of-the-art technology designed for deep space missions, yet the introduction of certain scientifically justified standards as the very basis for the rough selection of base locations enhance and concentrate our outlook to sites that pose an influence over much of the key aspects of the mission objectives. Therefore, appertaining to the recommendations put-forth in a conference at the Lunar Planetary Institute (LPI) [41], we propose the factors that are instrumental in the final selection of the best sites, tailored for the important pre-requisites of the mission in question.

As a starting point, we classify the mission architecture into two stages, which are compatible with the varied types of lunar missions conducted by NASA and other space agencies.

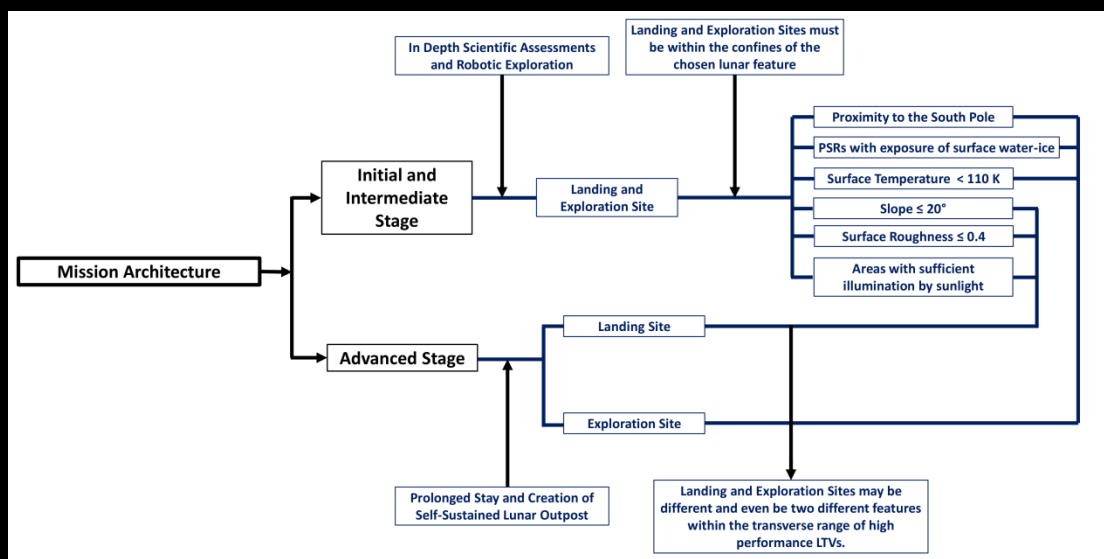


Figure 39: A generalized mission architecture.

The missions belonging to former class, are being termed as *Initial and Intermediate Stage missions*, due to the fact that lunar expeditions to be conducted in the near-future combine the two sub-stages into a multitude of mission objectives. At the *Initial Stage*, the focus is on conducting robotic

missions to gather essential data and perform preliminary assessments. These missions are aimed at understanding the lunar environment, identifying potential resources, and assessing the feasibility of human exploration. Robotic landers and rovers may be deployed to study the lunar surface, analyze soil samples, map the terrain, and collect data on radiation levels and environmental conditions. These missions provide crucial groundwork and scientific insights to inform future endeavors. The *Intermediate stage* incorporates human missions and this phase involves sending astronauts to the lunar surface for extended stays and in-depth scientific research. Astronauts would conduct experiments, deploy more advanced instruments, and establish scientific outposts or habitats. The focus shifts to understanding long-duration human presence on the Moon, testing technologies for resource utilization and life support systems, and developing the necessary infrastructure for sustained exploration. This stage also enables the evaluation of potential landing sites for future missions. Thus, both the stages combined form the basis of the establishment of sustainable lunar habitats. In the fully prepared and *Advanced Stage* of Moon exploration, the objective is to establish a sustainable lunar presence and enable more ambitious missions. This includes constructing permanent lunar bases or habitats that can support long-term human habitation. Advanced infrastructure, such as power generation systems, in-situ resource utilization capabilities, and 3D printing technologies, would be implemented to create a self-sufficient and productive lunar outpost. Additionally, the focus may shift towards utilizing the Moon as a staging point for deeper space exploration, such as missions to Mars and beyond.

For missions designed for *Initial and Intermediate Stages* (the paramount focus for this report), the landing sites and the sites of exploration have been suggested to be associated to the chosen lunar feature, based on the prior works on the subject and early stage safety parameters. For advanced staged missions, the sites can be chosen to be distant to some extent, but not ignorant of the aspect of the performance of the highly sophisticated Lunar Terrain Vehicles (LTVs). Therefore, for the former stages which encompass the primary concerns of missions such as Artemis III and the Chang'e Project, we utilize the same principles of zonal division, analogous to the crater selection, intended for the similar selection of landing/exploration sites.

Similar to the algorithm for craters, we categorize the generalized candidate locations (also based on our prior analyses on different lunar features) into three

zones, namely, Zones I, II and III, with priorities depending upon the constraints.

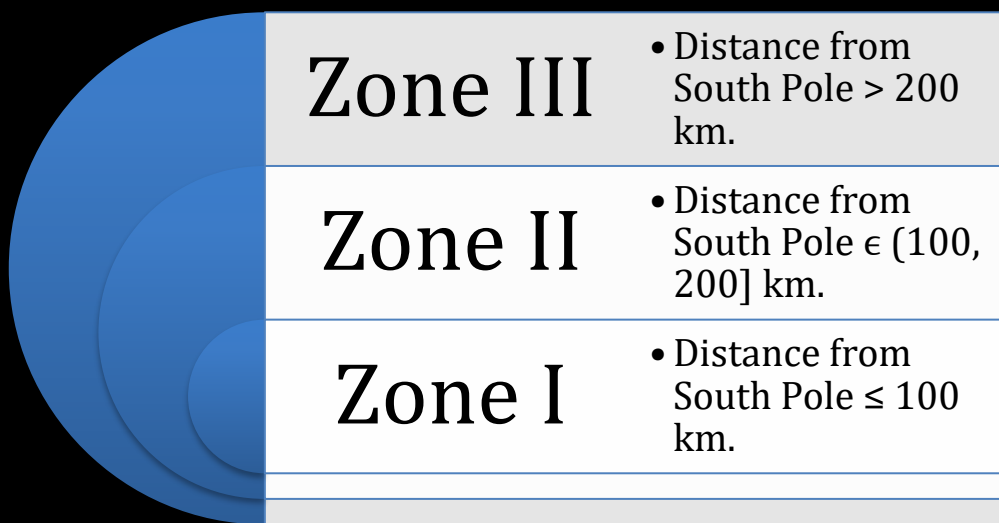


Figure 40: Zonal Division of potential base locations.

The choice of the thresholds were presented based on the incorporation of nominated sites and to maintain a synchronous distribution of locations at par with the ongoing lunar missions. Since the former stage confines its targets within the Zone I locations, therefore prompt attention must be given to those candidate sites while slowly progressing towards the majority of the distant ones, i.e. locations categorized under Zones II and III.

Summarizing the results of the initial analyses, it is quite evident that the entirety of Zone I candidate locations belong to the family of craters, more specifically the instances falling into the Primary Zone of crater selection. But in order to establish more robust arguments towards the selection of the most suitable locations, we need to employ certain conditionals as has also been stated at the start of this section. These conditions, with reference to prior literature boils down to four major criteria, the first major one being the proximity to the lunar south pole. The second criteria, being the slope criteria, ensures that landing modules are not exceeding a 20 degree tilt which could cause issues with instrument performance and prevents the lander from possibly falling on its side, while also ensuring terrain traversability for a potential rover [41]. The next criterion address the safety concerns by addressing the surface roughness. In order for a site to be considered “safe”, the area must be free of boulders larger than 1 m in diameter. Since block distribution data from LRO’s Diviner instrument is not available for the lunar south pole, another

option to assess boulder and crater distributions on the surface is to use roughness maps which help express the elevation differences between a central pixel and its neighboring eight pixels (a.k.a cells). Roughness is defined as the largest inter-cell difference of a central pixel and its surrounding eight cells. Roughness maps were produced from the 5 mpp and 10 mpp LOLA DEMs. High values represent more rugged and rough terrain (large boulders, steep dropoffs, etc.) whereas low values represent smoother, more level surfaces. Roughness values of 0.4 m (40 cm) and less were used for this site selection to help avoid undesired lander tilt and other safety concerns [41]. The next successive condition emerges in the form of surface temperatures. Since there is a very specific cutoff for ice sublimation temperature at less than 110 K [41], therefore we propose the choice of sites with presence of areas within that temperature range. Finally, besides the inevitable aspect of the existence of PSRs with presence of water-ice and other volatiles, the presence of regions with enough illumination by sunlight makes the chosen location more suited for the installation of solar panels and establishment of base habitats.

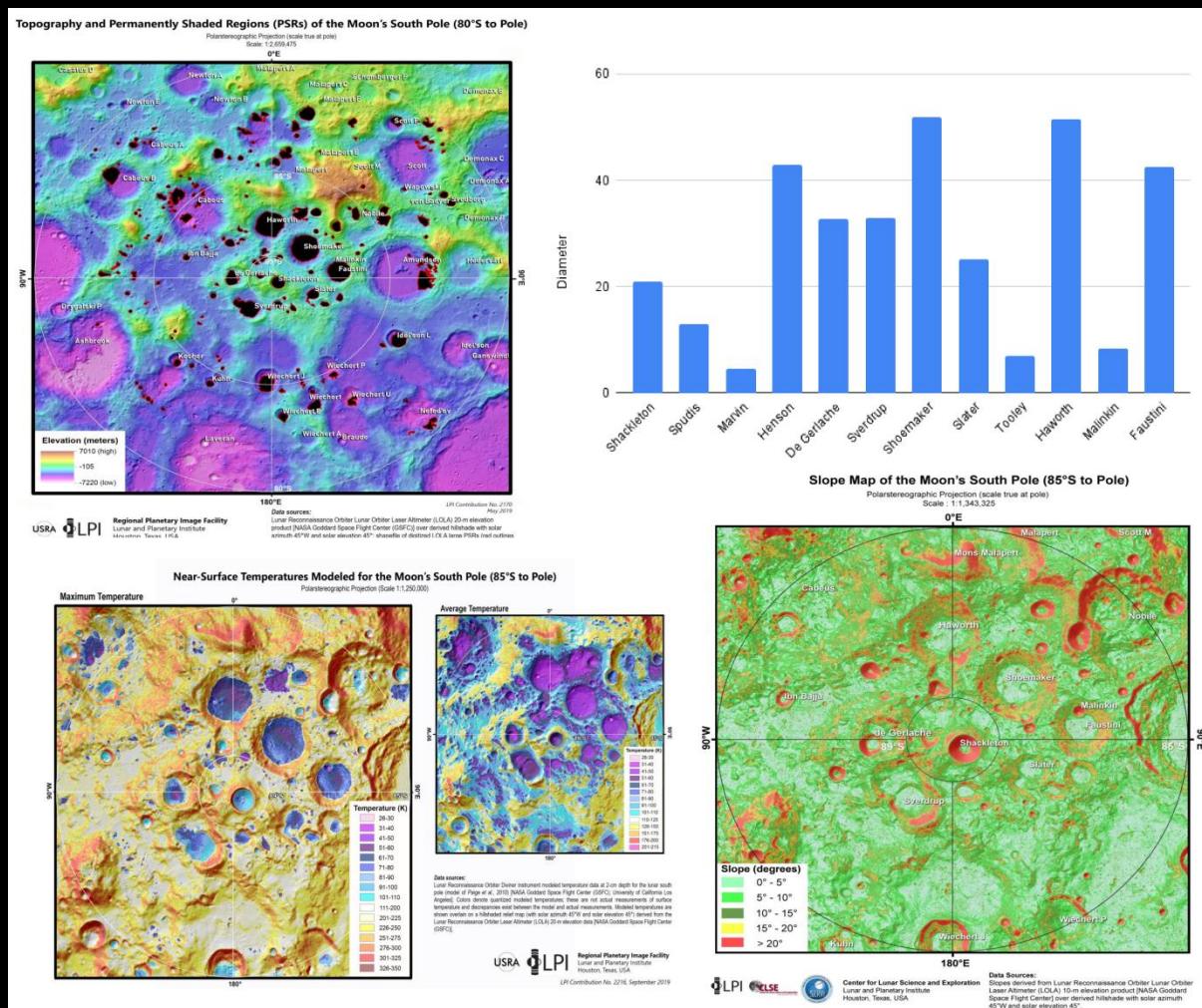


Figure 41: The Lunar South Pole Topographic, PSRs & Slope Maps and Near-Surface Temperatures Modeled for the Moon's South Pole (85°S to Pole) [49].

Therefore based on the aforementioned conditions critical towards the effective selection of the ideal spots, we therefore turn towards the data and extremely detailed maps produced by the the Lunar Planetary Institute on top of the information beamed back to Earth by the ongoing lunar missions. To begin with the immensity of the Primary Zone craters, the five largest craters (in terms of their diameters as depicted in Fig. 41.) which come up are *Shoemaker*, *Haworth*, *Henson*, *Faustini* and *Sverdrup*. But due to the larger extent of PSR region within the Sverdrup crater compared to crater Henson, we prioritize the four craters Shoemaker, Haworth, Faustini and Sverdrup to be evaluated for multi-facet advantages, especially due to the presence of the large regions of permanent shadow and in-turn, comprising of the highest concentrations of surface water-ice exposures [41]. With reference to the near surface temperature modelling and he slope map of the lunar south pole, all four of these craters have large portions (especially the PSRs) of their approximately flat crater floors have temperatures below the chosen upper bound of 110 K. Furthermore, the walls of these craters have sections with slopes within the range of 15 to 20 degrees, thus enabling the computation of possible travel routes for rovers and even astronauts to reach the depths of the craters. Hence, with the introduction of priority zones, the four above mentioned craters rise up to be the most important ones in terms of initial exploration. Shackleton, although possessing the apt potential to be a location of top priority only falls short of the fact that it has nearly vertical walls and the crater floor has a much higher degree of surface roughness. Yet, with advanced instrumentation and cutting-edge engineering, the crater is most likely to be a major target site for exploration and with the speciality of it being a treasure-trove of valuable insights into past lunar geological activities, the well-preserved Shackleton crater is therfore a top-priority candidate despite all the odds. As a sidenote, this report focuses every feature from an exploratory viewpoint, therefore every selection deals with the potential feasibility and importance of venturing the locations that we choose, and thereby suggesting the creation of bases in close proximity to the feature (such as the crater rim, on a nearby massif, etc.), the precise nature of which (inclusive of the landing) shall be discussed in subsequent documentation.

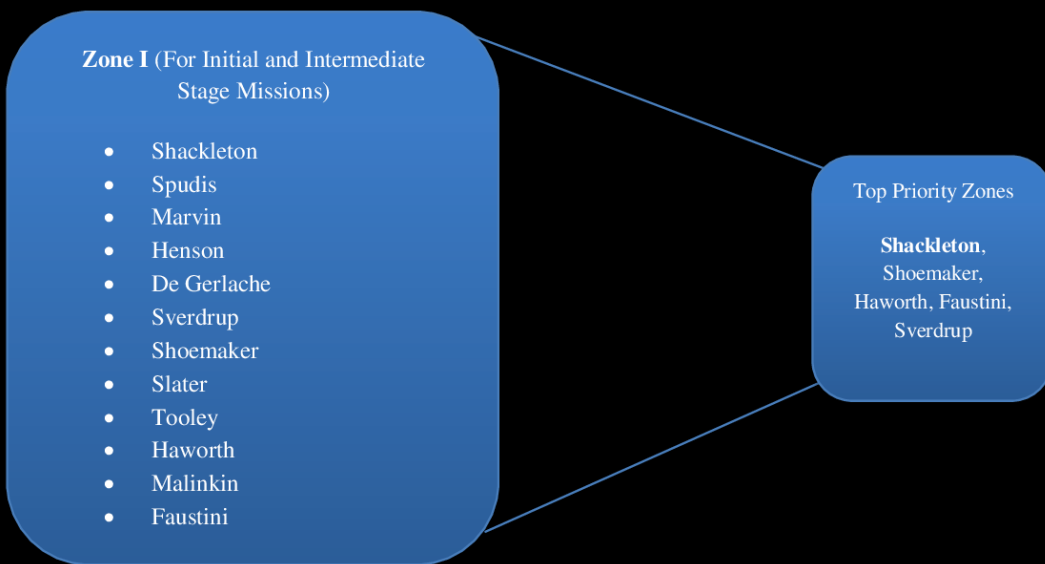


Figure 42: Top Priority Zones for Initial & Intermediate Stage Missions.

Besides the four top priority zones that have been analyzed in the preceeding anecdote, the other nominated sites in Zone I are equally worth exploration and perhaps base creation depending on the surrounding terrain and conditions that favor extended sustainability. With the transition to advanced stages, we would have the complete potential to envision the construction of habitats in virtually every potential site and with more intense scientific research added to the greater possibility of ISRU, humanity would achieve a major milestone towards emerging as an inter-planetary species and even beyond.

Data Availability: All the data and software available for this analysis can be downloaded from <https://github.com/Prithwis-2023/Moon-Base-Project>. For additional information regarding data sharing, please email at jonathan.h.jiang@jpl.nasa.gov.

Contributors:

- **Dr. Jonathan H. Jiang** (Jet Propulsion Laboratory, California Institute of Technology, Pasadena, CA, USA)
- **Prithwis Das** (Vivekananda Mission High School, WB, India)
- **Derek Zuo** (Sage Hill School, Newport, CA, USA)

References:

- [1] Tabor, A. (2018, August 17). *Ice confirmed at the Moon's Poles*. NASA. <https://www.nasa.gov/feature/ames/ice-confirmed-at-the-moon-s-poles>
- [2] Buratti, B. J. (2004, June 17). *Moon*. Encyclopedia of Physical Science and Technology (Third Edition). <https://www.sciencedirect.com/science/article/pii/B0122274105004609>
- [3] Wikimedia Foundation. (2022, May 14). *Mare Australe*. Wikipedia. https://en.wikipedia.org/w/index.php?title=Mare_Australe&oldid=1087821478
- [4] Meng, Z. G., Chen, S. B., Zheng, Y. C., Cheng, W. M., Zhu, Y. Q., Cai, Z. C., et al. (2020). Mare Deposits Identification and Feature Analysis in Mare Australe Based On CE-2 CELMS Data. *Journal of Geophysical Research: Planets*, 125, e2019JE006330. <https://doi.org/10.1029/2019JE006330>
- [5] *Digital Lunar Orbiter Photographic Atlas of the moon, database*. Lunar and Planetary Institute (LPI). (n.d.). https://www.lpi.usra.edu/resources/lunar_orbiter/bin/srch_nam.shtml
- [6] UCLA. (2022, May 10). *New diviner data product of the Lacus Mortis Region released*. Diviner. <https://www.diviner.ucla.edu/single-post/new-diviner-data-product-of-the-lacus-mortis-region-released>
- [7] Liu, J., Liu, J., Yue, Z., Zhang, L., Wang, J., & Zhu, K. (2022, February 22). *Characterization and interpretation of the global lunar impact basins based on remote sensing*. Icarus. <https://www.sciencedirect.com/science/article/abs/pii/S0019103522000720>
- [8] Fassett, C. I., Head, J. W., Kadish, S. J., Mazarico, E., Neumann, G. A., Smith, D. E., and Zuber, M. T. (2012), Lunar impact basins: Stratigraphy, sequence and ages from superposed impact crater populations measured from Lunar Orbiter Laser Altimeter (LOLA) data, *J. Geophys. Res.*, 117, E00H06, doi:[10.1029/2011JE003951](https://doi.org/10.1029/2011JE003951).
- [9] Liu, J., Liu, J., Yue, Z., Zhang, L., Wang, J., & Zhu, K. (2022, February 22). *Characterization and interpretation of the global lunar impact basins based on remote sensing*. Icarus. <https://www.sciencedirect.com/science/article/abs/pii/S0019103522000720>

[10] *The Moon's major impact basins*. The Planetary Society. (n.d.).
<https://www.planetary.org/space-images/lunar-impact-basins>

[11] *Lunar Orbiter: Impact basin geology*. Lunar and Planetary Institute (LPI). (n.d.-b).
https://www.lpi.usra.edu/lunar/missions/orbiter/lunar_orbiter/impact_basin/

[12] *Planetary names*. Planetary Names. (n.d.).
<https://planetarynames.wr.usgs.gov/>

[13] Wikipedia contributors. "Planitia Descensus." *Wikipedia, The Free Encyclopedia*. Wikipedia, The Free Encyclopedia, 24 Feb. 2022. Web. 24 Dec. 2022.

[14] Wikipedia contributors. "Promontorium Kelvin." *Wikipedia, The Free Encyclopedia*. Wikipedia, The Free Encyclopedia, 24 Feb. 2022. Web. 25 Dec. 2022.

[15] Crater chains on the Lunar South Pole - lpi.usra.edu. (n.d.).
<https://www.lpi.usra.edu/exploration/education/hsResearch/presentations/posters/BellaireHSJuniors.pdf>

[16] October 1, 2014 Media contact: Kevin Stacey 401-863-3766. (2014, October 1). *Origin of moon's “ocean of storms” revealed*. Origin of Moon's “ocean of storms” revealed | News from Brown.
<https://news.brown.edu/articles/2014/10/moon>

[17] *Edge of oceanus procellarum*. ESA. (n.d.).
https://www.esa.int/ESA_Multimedia/Images/2006/06/Edge_of_Oceanus_Procellarum

[18] Bailey, A. (n.d.). *Rilles and rilles: Sinuous, straight, and arcuate*. Rilles and Rilles: Sinuous, Straight, and Arcuate. <https://www.lroc.asu.edu/posts/1147>

[19] R, C. C., & R, H. B. (1988, April 5). *A Preliminary Survey of Lunar Rilles: The Search for Intact Lava Tubes*. 1988LPICo.652...58C page 58.
<https://adsabs.harvard.edu/full/1988LPICo.652...58C>

[20] Dunbar, B. (n.d.). *Rupes Recta*. NASA.
https://www.nasa.gov/mission_pages/LRO/multimedia/lroimages/lroc-20110209-rupes.html

- [21] Hoover, R. (2023, February 13). *Moon Mountain name honors NASA mathematician melba mouton*. NASA.
<https://www.nasa.gov/feature/ames/moon-mountain-name-honors-nasa-mathematician-melba-mouton>
- [22] *The Moon*. Valleys | Moon | Space FM. (n.d.).
<https://www.space.fm/astronomy/earthmoonsun/valleys.html>
- [23] Wikipedia contributors. "Vallis Schrödinger." *Wikipedia, The Free Encyclopedia*. Wikipedia, The Free Encyclopedia, 28 Aug. 2021. Web. 9 May. 2023.
- [24] Horvath, T., Hayne, P. O., & Paige, D. A. (2022). Thermal and Illumination Environments of Lunar Pits and Caves: Models and Observations From the Diviner Lunar Radiometer Experiment. *Geophysical Research Letters*, 49(14), e2022GL099710. <https://doi.org/10.1029/2022GL099710>
- [25] Steigerwald, B. (2022, July 25). *NASA's LRO finds Lunar Pits Harbor comfortable temperatures*. NASA.
<https://www.nasa.gov/feature/goddard/2022/lro-lunar-pits-comfortable>
- [26] *Shaping the planets: Impact cratering*. Lunar and Planetary Institute (LPI). (n.d.-c).
https://www.lpi.usra.edu/education/explore/shaping_the_planets/impact-cratering/
- [27] NASA. (n.d.). *Catalog page for PIA00001*. NASA.
<https://photojournal.jpl.nasa.gov/catalog/?IDNumber=PIA00001>
- [28] *Lunar reconnaissance orbiter camera*. Pits Atlas | Lunar Reconnaissance Orbiter Camera. (n.d.). <https://www.lroc.asu.edu/pits/list>
- [29] Clavius crater water - USRA. (n.d.-a).
<https://www.hou.usra.edu/meetings/lpsc2021/pdf/1411.pdf>
- [30] Potter, S. (2020, October 26). NASA's Sofia discovers water on sunlit surface of Moon. NASA. <https://www.nasa.gov/press-release/nasa-s-sofia-disCOVERS-water-on-sunlit-surface-of-moon>
- [31] Milani, Hady & Calzada-Diaz, Abigail & Hettrich, Sebastian & De Quattro, Nicola & Antonello, Andrea & D., Bielicki. (2016). Alcides: A Novel

Lunar Mission Concept Study For The Demonstration Of Enabling Technologies In Deep-Space Exploration And Human- Robots Interaction.

[32] Dominov, E., & Mest, S. C. (n.d.). *40th lunar and planetary science conference (2009)* . GEOLOGY OF ANTONIADI CRATER, SOUTH POLE AITKEN BASIN, MOON. .

<https://www.lpi.usra.edu/meetings/lpsc2009/pdf/1460.pdf>

[33] NASA. (n.d.-b). *Lunar Orbiter Laser Altimeter*. NASA.

<https://lunar.gsfc.nasa.gov/lola/feature20110415.html>

[34] Wayback Machine. (n.d.).

<https://web.archive.org/web/20181005195534/http://www.lpod.org/cwm/DataStuff/Lunar%20Basins.htm>

[35] NASA. (n.d.). *Shackleton Crater's Illuminated Rim & Shadowed interior – moon: NASA science*. NASA. <https://moon.nasa.gov/resources/483/shackleton-craters-illuminated-rim-shadowed-interior/>

[36] Zuber, Maria, et al. "Constraints on the Volatile Distribution within Shackleton Crater at the Lunar South Pole." *Nature*, vol. 486, no. 7403, 2012, pp. 378-381, <https://doi.org/10.1038/nature11216>. Accessed 29 May 2023.

[37] Dunbar, B. (n.d.). *Researchers estimate ice content of crater at moon's south pole*. NASA. https://www.nasa.gov/mission_pages/LRO/news/crater-ice.html

[38] Magazine, S. (2021, December 1). *Moon Crater Spudis*. Smithsonian.com. <https://www.smithsonianmag.com/air-space-magazine/moon-crater-spudis-180979373/>

[39] IAU Task Group . (2021, September 1). *Henson crater lunar south polar region - lunar and planetary institute ... Henson Crater*. <https://www.lpi.usra.edu/features/092021/crater/henson-crater-lunar-south-pole-details.pdf>

[40] Magazine, S. (2021a, December 1). *Moon Crater Spudis*. Smithsonian.com. <https://www.smithsonianmag.com/air-space-magazine/moon-crater-spudis-180979373/>

- [41] Landing site analysis for a lunar polar water ice ground truth ... - USRA. (n.d.). <https://www.hou.usra.edu/meetings/lunarsurface2020/pdf/5120.pdf>
- [42] Lunar Crater observing and sensing satellite site selection 9001. (n.d.-b). <https://www.lpi.usra.edu/meetings/lcross2006/pdf/9001.pdf>
- [43] *Lunar Crater named for former SWRI space scientist David C. Slater.* Southwest Research Institute. (2017, April 7). <https://www.swri.org/press-release/lunar-crater-named-former-swri-space-scientist-david-c-slater>
- [44] Hille, K. (2021, January 26). *The naming of Tooley crater.* NASA. <https://www.nasa.gov/feature/goddard/2021/the-naming-of-tooley-crater/>
- [45] Thermal extremes in permanently shadowed regions at the Lunar South Pole. (n.d.-c). <https://www.lpi.usra.edu/meetings/lpsc2013/eposter/2617.pdf>
- [46] Dunbar, B. (n.d.-b). *South-Polar First look.* NASA. https://www.nasa.gov/mission_pages/Mini-RF/news/2009-01-16_south_polar.html
- [47] Wikipedia. (n.d.). *Malinkin.* Wikidata. <https://www.wikidata.org/w/index.php?title=Q21660743&oldid=1373460553%3E>.
- [48] Brown, H. M., Robinson, M. S., & Boyd, A. K. (2020). *Morphologic landforms in Shoemaker and Faustini Lunar ... - USRA.* MORPHOLOGIC LANDFORMS IN SHOEMAKER AND FAUSTINI LUNAR PERMANENTLY SHADOWED CRATERS. <https://www.hou.usra.edu/meetings/lpsc2020/pdf/1765.pdf>
- [49] Stopar , J. D., & Kring, D. A. (n.d.). *Lunar South Pole Atlas.* Lunar and Planetary Institute (LPI). <https://www.lpi.usra.edu/lunar/lunar-south-pole-atlas/>

